Quantifying the dynamics of COVID-19 burden and impact of interventions in Java, Indonesia

Bimandra A Djaafara[1,2], Charles Whittaker[1], Oliver J Watson[1], Robert Verity[1], Nicholas F Brazeau[1], Widyastuti[3], Dwi Oktavia[3], Verry Adrian[3], Ngabila Salama[3], Sangeeta Bhatia[1], Pierre Nouvellet[1,4], Ellie Sherrard-Smith[1], Thomas S Churcher[1], Henry Surendra[2], Rosa N Lina[2], Lenny L Ekawati[2], Karina D Lestari[2], Adhi Andrianto[2], Guy Thwaites[5,6], J Kevin Baird[2,6], Azra C Ghani[1], Iqbal RF Elyazar[2], Patrick GT Walker[1]

[1]MRC Centre for Global Infectious Disease Analysis, Department of Infectious Disease Epidemiology, Imperial College London, London, United Kingdom

[2]Eijkman-Oxford Clinical Research Unit, Jakarta, Indonesia

[3]Jakarta Provincial Department of Health, Jakarta, Indonesia

[4]School of Life Sciences, University of Sussex, Brighton, UK

[5]Oxford University Clinical Research Unit, Ho Chi Minh City, Vietnam

[6]Centre for Tropical Medicine and Global Health, Nuffield Department of Medicine, University of Oxford, Oxford, UK

Correspondence to: ielyazar@eocru.org and patrick.walker@imperial.ac.uk

Abstract

Measuring COVID-19 spread remains challenging in many countries due to testing limitations. In Java, reported cases and deaths increased throughout 2020 despite intensive control measures, particularly within Jakarta and during Ramadan. However, underlying trends are likely obscured by variations in case ascertainment. COVID-19 protocol funerals in Jakarta provide alternative data indicating a substantially higher burden than observed within confirmed deaths. Transmission estimates using this metric follow mobility trends, suggesting earlier and more sustained intervention impact than observed in routine data. Modelling suggests interventions have lessened spread to rural, older communities with weaker healthcare systems, though predict healthcare capacity will soon be exceeded in much of Java without further control. Our results highlight the important role syndrome-based measures of mortality can play in understanding COVID-19 transmission and burden.

Main Text

Following the first reports of a novel virus from Wuhan, China, in December 2019 (*1*), SARS-CoV-2 has spread rapidly around the world, leading to more than 30 million confirmed cases of associated coronavirus disease (COVID-19) and over 900,000 reported deaths in 216 countries as of 20th September 2020 (*2*). Measuring the rapid spread of COVID-19 has been challenging across the world due to the high fraction of asymptomatic infections (*3*) and limitations in testing capacity (*4*, *5*). Mortality attributed to COVID-19 is widely considered to be a more reliable metric to measure epidemic trajectory (*6*). However, even in countries with well-resourced health and surveillance systems, accurate measurement of the incidence of death has proven problematic due to the high number of deaths occurring outside of hospitals and uncertainty in attributing cause of death (*7*). These problems are more

acute in Upper and Lower Middle-Income Countries (UMICs, LMICs), where health system reporting may become overwhelmed (*4*, *8–13*).

Interpreting trends in both cases and deaths from COVID-19 is vital to understanding the dynamics of transmission, the burden of disease, and the range of future trajectories of the epidemic. Here we seek to better understand the epidemic in Indonesia, a nation of 274 million people reporting the second-highest number of cases (244,676 as of 20th September, behind only the Philippines) and the heaviest death toll (9,553 reported deaths as of 20th September) among Southeast Asian countries (*2*, *14*). To do so, we utilise a diverse range of data sources, including COVID-19 protocol (C19P) funeral data, as an indirect indicator of syndromic-based mortality and population mobility estimates at a variety of spatial scales. These are then integrated within a meta-population mathematical model of transmission to better understand and quantify the dynamics of the COVID-19 epidemic. Specifically, we focus on the island of Java, where 56% of Indonesians live and from which 59% of cases and 66% of deaths have been reported (**Figure 1**). We use these data to explore possible future trajectories of the epidemic on the island and the extent to which remaining data limitations contribute to uncertainty within these projections.

Observed Spread of COVID-19 Across Java and Indonesia

As of 20th September 2020, there had been a total of 244,676 reported cases and 9,553 deaths in Indonesia (*14*). The first reported cases of COVID-19 in the country were from two residents of Depok, in West Java province on 2nd March 2020, although there had been concern that the disease had been circulating widely prior to this date (*15*, *16*). Both cases were transferred for treatment to a specialist infectious disease hospital in Jakarta (*17*). The city of Jakarta subsequently became the epicenter of the epidemic in the country, accounting for a large fraction of the country's known COVID-19 burden (25% and 16% of cases and deaths respectively up to 20th September 2020), and prompting the implementation of a variety of non-pharmaceutical interventions (NPIs) as cases and deaths rose in the city during March and April. These included national social distancing measures encouraging people to work, study and worship at home (15th March) (*18*); mandated social distancing measures implemented on 10th April as part of a regional lockdown in Jakarta named *Pembatasan Sosial Berskala Besar* (PSBB) in Indonesian and subsequently extended to the other parts of the Jakarta metropolitan area a few days later (*18*); and a ban on domestic travel to prevent the annual migration of the population to home villages to celebrate the festival of Eid during the month of Ramadan (24th April to 7th June) (*19*). On 5th June, the city of Jakarta entered the transitional PSBB period, where some restrictions implemented during the PSBB were relaxed (*20*). In late June, Indonesia entered *Adaptasi Kebiasaan Baru* (AKB or 'the new normal') period where partial lifting of the PSBB measures was implemented, allowing companies, restaurants, and malls to resume their activities in compliance with Ministry of Health protocols and at half-capacity (these milestones are illustrated in **Figures 1A and 1B**) (*18*). Following this lifting of restrictions, daily COVID-19 cases and deaths have increased progressively across Indonesia with significant subnational spread to all 34 provinces, with community transmission evident across the six provinces of Java (**Figures 1C and 1D)**. At the time of this study, PSBB has been scheduled for reimplementation within Jakarta on 14th of September as an emergency measure to protect healthcare delivery capacities (*21*).

Understanding Initial Establishment, Transmission and Dynamics of SARS-CoV-2 in Jakarta

In order to understand emerging COVID-19 trajectories across Indonesia, we first sought to understand the initial dynamics and transmission of the virus in the city of Jakarta, an urban city with a population of

over 9 million and the main epicentre of the virus in Indonesia during early 2020. Three epidemiological indicators of COVID-19 obtained from (*22*) are used - reported cases, reported deaths of individuals confirmed to be COVID-19 positive prior to death, and the daily reported COVID-19 protocol (C19P) funerals. C19P funerals are conducted when, at the time of death, the deceased were either COVID-19 positive or had COVID-19 symptoms and were either yet to be tested or to receive results. **Figure 2A** shows the daily reported cases, deaths, test positivity ratios, and funerals with C19P in Jakarta. These data are transformed into inferred dates of symptom onset using estimates of the delays between onset and diagnosis, onset and death, and onset and funeral derived from anonymised individual-level data from confirmed COVID-19 patients in Jakarta (**Figure 2B**, also see **Methods** and **Supplementary Figure S1**). As of 2nd March, when COVID-19 was first identified in Indonesia, we estimate that 31 (22-41 95% CrI) and 124 (107-139 95% CrI) confirmed deaths and C19P funerals (assuming all funerals represent deaths due to COVID-19) had symptom onset occurring before 2nd March. Assuming an infection fatality ratio of 0.657%, estimated from China (*23*) and adjusted for the population age-structure in Jakarta, we estimate 7,920 (5,490-10,360 95% CrI) infections based on confirmed deaths (reflecting an assumption that all undiagnosed individuals with a C19P funeral would have tested negative) or 30,830 (26,550-34,960 95% CrI) based on C19P funerals (reflecting an assumption that all undiagnosed individuals with a C19P funeral would have tested positive) had occurred in Jakarta by 2nd March. This suggests both substantial undetected initial transmission across the city as well as large discrepancies in the predicted burden of COVID-19 depending on the data source used.

Estimates of the virus' dynamics and transmissibility are also sensitive to the data source utilised. Based on reported cases, we predict the epidemic to have peaked around mid-April, before rising again in September 2020 to a far higher level than previously experienced in Jakarta (**Figure 2B**). The test-positivity rate declined in the first half of 2020, indicating increased testing rates and case-ascertainment, which further complicate interpretation of trends based on case data alone. The effects of this bias are visible when contrasted with the data on C19P funerals, which suggest the peak in infections likely occurred in mid-March, and that current infection levels are only now at levels comparable to their initial peak. The epidemic trajectory suggested by the officially reported deaths (requiring a positive COVID-19 test), which are also likely to be biased by changes in testing rates but to a lesser extent than cases, fall between those of cases and C19P funerals.

To better quantify and understand the dynamics of spread within Jakarta, we utilise a branching-process based methodology to generate estimates of the reproduction number over time (R_t) (*24*). Three different estimates are obtained based on the three reconstructed time-series of symptom-onset derived from cases, deaths, and C19P funerals. All support the substantial impact of NPIs: we estimate R_t to be between 1.5 and 2.5 initially, subsequently declining to below 1 during the PSBB period followed by a more recent increase to slightly above 1 as Jakarta entered the transitional PSBB in early June (**Figure 2C**). These estimates all show strong and significant correlation (0.91, 0.73, and 0.92 for cases, deaths, and C19P funerals respectively, all with $p<0.001$) with observed mobility patterns as measured by Google Mobility Reports (*25*) (**Figure 2D**). However, estimates based upon funeral trends support a more rapid, larger, and more sustained impact of interventions than those based upon case-reporting (which are most likely to be affected by biases associated with improved testing and ascertainment). The correlation with within-city mobility is lowest for the deaths data, where substantial variation in day-to-day death reporting leads to more unstable estimates of R_t over time.

Calculating the correlation between mobility and R_t before and after the AKB ("new-normal") period suggests a decoupling between transmission and mobility (as observed across other settings e.g., in

China (*26*)), whereby estimates of R_t during periods of equivalent levels of mobility during AKB are lower than estimates obtained prior to AKB (**Supplementary Figure S3**).

Understanding COVID-19 Risk and Subnational Spread of SARS-CoV-2 Across Java

We next sought to understand the dynamics of the epidemic's subsequent subnational spread across the six provinces of Java and explore how fine-scale heterogeneity in factors relevant to COVID-19 risk and transmission might influence the burden of the disease (including demography, healthcare capacity, and between-district mobility). Our results highlight substantial variation across the island in these risk factors, with the proportion of individuals over the age of 50 (**Figure 3A**, an age above which the risk of COVID-19 mortality markedly increases (*23*)) varying by over 2.5-fold between districts, as well as substantial variation in the number of hospital beds per 1 thousand population. This latter difference is most pronounced when comparing the comparatively well-resourced Jakarta setting (2.22 beds per thousand population) to the poorer, more rural setting of Tasikmalaya in West Java (0.18 beds per thousand population) (**Figure 3B**). Patterns of between-district mobility outside of the window of the pandemic, estimated using mobile phone data over the period of 1st May 2011 - 30th April 2012, highlight the extent to which these settings are connected. Between-district connectivity is particularly high during the Ramadan period, which is marked by the large-scale movement of the population from densely populated Jakarta to other more rural and less well-resourced regions where populations are typically older and thus more vulnerable to morbidity and mortality as a result of COVID-19 infection (**Figures 3C** and **3D**).

In the absence of equivalent resolution C19P funeral data in other provinces, we applied our estimates of the relationship between mobility and R_t obtained from Jakartan funeral data (**Figure 3E**) to trends in Google Mobility data from the remaining provinces in Java. These estimates indicate a large impact on transmission in all provinces coinciding with the PSBB period. However, they also suggest that only in Jakarta and Yogyakarta were measures sufficient to bring R_t below 1 for a sustained period of time. Across all provinces, however, increases in mobility occurred either during early May (Banten, West Java, Central Java, and East Java) or alongside the establishment of the AKB in June (Jakarta and Yogyakarta), leading to corresponding increases in our estimates of R_t (**Figure 3F**).

To capture the subnational spread of the virus, we developed a meta-population model of SARS-CoV-2 transmission by extending an existing non-spatial model (*28*), with each population in the model representing either the city of Jakarta or one of the 113 remaining districts across Java. We parameterised the model using mobile phone data derived estimates of between-district mobility (during both Ramadan and non-Ramadan periods, **Figures 3C and 3D**) prior to the pandemic, data on district-level demographic structure, and our estimates of within-province R_t. **Figure 4A** shows the district-level metapopulation model-based simulation results for COVID-19 deaths for our baseline scenario designed to capture COVID-19 dynamics in Java to date, with the model calibrated to match patterns of mortality in Jakarta by varying the degree of initial seeding of infection early in January. **Table 1** shows a comparison between simulated trends in provinces outside of Jakarta for our model to both data on confirmed deaths and two additional, but incomplete, data sources for suspected deaths (a combination of both confirmed and probable COVID-19 deaths) in these provinces. These were weekly situation reports compiled by WHO (*18*), which provide estimates of suspected deaths from 13th May onwards; and estimates of cumulative suspected deaths based on provincial COVID-19 data monitoring website compiled by an independent group KawalCOVID19 (*29*). Given our simplified assumption of a consistent relationship between mobility and R_t across the island and uncertainties within the underlying levels of true Covid-19 mortality each dataset represents, we do not expect an exact match to any of these data.

However, the model appears to capture the approximate magnitude and timing of deaths across provinces during the PSBB period, with the epicenter shifting over time from Jakarta to satellite towns and other provincial capitals, and with Yogyakarta remaining least affected. Prior to the first week in June, the point of transition to the AKB, 'new-normal' period, our median baseline model estimates fall within the range between confirmed and suspected deaths of both WHO and provincial data in most provinces, with total suspected deaths falling well within the uncertainty bounds of the model for all provinces **(Table 1)**.

In addition to this baseline scenario (Scenario 1), we use our model to explore an additional four counterfactual scenarios across the six provinces (**Figure 4B**). These include a scenario assuming no movement reductions during the Ramadan period and similar R_t values to our baseline (Scenario 2); a scenario assuming no movement reductions during the Ramadan period and R_t values that are 75% of each district's R_0 value (Scenario 3); a scenario assuming no movement reductions during the Ramadan period and R_t values equal to each district's R_0 value (Scenario 4); and an unmitigated scenario assuming no implementation of interventions across the course of the epidemic (Scenario 5). In total, our baseline scenario produces an estimated 3,700 (1,500-7,390, 95% uncertainty interval (UI)) deaths up to May 31st. This provides an estimate of 71,250 (34,400-136,000, 95% UI) deaths averted when compared to an effectively unmitigated epidemic with R_t = 2 throughout this period (which we estimate would have resulted in 74,990 (36,360-142,750, 95% UI)) deaths). This number does not take into account the effects of healthcare services becoming overwhelmed (as shown by the negative values of the median number of hospital beds available per COVID-19 case needing hospitalisation under the unmitigated epidemic scenario, **Figure 4C**) on both direct and indirect mortality, an impact which would likely have been sizable given the wider spread to more rural settings with more scarce healthcare provision in our unmitigated scenario (**Figures 4D** and **4E**). Our estimates also suggest that the relatively aggressive Ramadan travel restrictions are likely to have had a sizable impact on preventing wider spread to more vulnerable rural areas.

Our baseline model (Scenario 1) increasingly over-predicts deaths in most provinces during the transitional PSBB and AKB 'new-normal period'. This is in line with our results suggesting a decoupling of within-province mobility from virus transmissibility over that period (observed across other settings (*26*), which could be related to individual-level changes in population behaviour such as increased mask-wearing, social distancing, changing work patterns, etc.). The reported cases in Jakarta substantially differ from model estimates after the AKB (**Supplementary Figure S4**), congruent with the province altering its testing strategy to more actively find cases and clusters of cases that include milder infections not requiring hospitalizations. Data from other provinces (which represent hospitalised cases only and do not include those identified through active case investigation) are more consistent with the model results.

Modelled Future Scenarios of COVID-19 Burden in Java

To better capture within-province transmission trends during the AKB and up to the present (and given current observed community spread in all provinces), we use the simpler non-spatial model to fit province-specific models to either reported deaths (from (*14*, *22*)) or both reported and suspected deaths (the C19P funerals data in the case of Jakarta (*22*) and collated from (*18*) otherwise, see **Methods** and **Supplementary Material**) (**Figure 5A**). Outside of Jakarta, model estimates of the attack rate (cumulative proportion infected) are below 5% across all provinces. In Jakarta, by contrast, the fitting was more sensitive to our choice of metric: fitting to all suspected deaths increasing the estimated attack rate by a factor of 4 to 14.0% (12.7-15.8%, 95% CrI), relative to the 3.5% (3.1-4.1%, 95% CrI) estimated when restricting analysis to confirmed deaths alone (**Figure 5B**). Irrespective of the data sourced used,

these estimates suggest attack rates across Java to be far short of putative herd immunity thresholds, with this threshold likely to range from 34.6% to 50% for an R_0 of 2 depending on assumptions surrounding heterogeneities in mixing and susceptibility (*30*). Moreover, our province-level point estimates for R_t between 20th August - 4th September ranged between 1.02-1.22 and 1.05-1.29 for confirmed and suspected deaths, respectively, indicating that burden is likely to continue to rise in the coming weeks.

We explore a range of future scenarios in each province using combinations of three values of the 'reproduction number under control', R_c, (i.e., the average number of secondary infections occurring from an index infection in a wholly susceptible population but accounting for the impact of currently implemented interventions): a 'current' scenario with R_c=1.25 to approximate the recent trajectory of the epidemic; a 'suppression' scenario where $R_c = 0.75$, designed to represent a scenario where changes in intervention measures are successful in achieving levels of control necessary to suppress transmission; and a 'return to normal' scenario where $R_c = 2.0$, representing levels of transmission estimated at the beginning of the epidemic. These scenarios, using a range of estimates of transmissibility already observed across Java to date, highlight how different assumptions about future changes in control-policy and population-level behaviour (and their subsequent impact on R_c) can produce a wide array of future epidemic trajectories **(Figure 5C)**. Extrapolating recent trends in transmission in Jakarta (i.e., our 'current' scenario) suggests a situation where demand for health services will increasingly approach, and likely exceed, capacity in the coming weeks or months **(Figure 5D)** but to a much lesser extent than would occur in circumstances where R_c further increased towards that estimated at the beginning of the epidemic (R_c of 2). This scenario is largely mirrored elsewhere in Java, where, on average, current levels of infection are lower but where dedicated healthcare services are in shorter supply. Our results suggest that attempts to further suppress transmission, such as the recent re-imposition of PSBB in Jakarta in recent days, if successful in reducing R_c below 1, could largely keep healthcare within capacity. However, this will not alleviate the need for the development of sustainable approaches to controlling transmission over the coming year: in both our current and suppression scenarios, we estimate returning to pre-pandemic levels of social interaction once burden has subsided to low levels (a 'Return to Normal' scenario, where $R_c = 2.0$ once burden has fallen below an average of 1 death per day over the course of a week) would risk a substantial subsequent, additional wave of infection across Java.

Our uncertainty in the underlying burden to date is also a key contributor to our uncertainty in the future trajectory of the epidemic, particularly in Jakarta, which has the highest disparity between confirmed and suspected deaths. For example, our projection of current trends assuming all suspected deaths are due to COVID-19 suggests an imminent threat of the health services reaching capacity within the city. In contrast, our projection based solely upon confirmed deaths would suggest healthcare will remain within the capacity for longer, due to lower levels of currently active infection. However, this epidemic trajectory results in a larger and more prolonged peak lasting well into 2021, driven by much lower levels of accumulated immunity within the population. If current attempts to achieve suppression are successful, this uncertainty is likely to be of even higher importance in terms of understanding the level of control required to prevent a subsequent wave: assuming all suspected deaths are due to COVID-19, our suppression scenarios achieve a level of immunity where current levels of R_c could be sustained without a major subsequent wave. By contrast, assuming only confirmed deaths are due to COVID-19 would imply much lower levels of immunity, producing a further subsequent wave in 2021 in our suppression scenario if R_c returned to current levels.

Conclusion

Our analysis highlights the challenges in capturing the transmission dynamics during an emerging pandemic of a novel pathogen. Basing our epidemiological inference on deaths (both diagnostically confirmed and using C19P funeral data as an indirect measure of symptomatically suspected), we estimate substantial circulation of SARS-CoV-2 in Jakarta prior to the date of the first confirmed COVID-19 case, as well as an earlier and more sustained decline in transmissibility in response to NPIs. In addition to the different dynamics of the reproduction number suggested when comparing inference using cases and deaths, we demonstrate that alternative sources of mortality data can help supplement our understanding of the historical spread of the epidemic. This is particularly evident in Jakarta, where the estimated attack rate varies by four-fold depending on the extent to which the deaths of individuals assessed to have been displaying COVID-19 symptoms but yet to receive a test result at the point of death (and subsequent burial) are assumed attributable to the infection.

This undiagnosed COVID-19 burden in Jakarta and spread to date has important consequences for our projections of the current trajectory of the epidemic and the likely longer-term impact of interventions such as the re-establishment of measures aimed at suppressing transmission in Jakarta in recent days. These results highlight the critical importance of placing recently observed COVID-19 dynamics within the context of previous patterns of the spread of the disease to more accurately understand the future. In many settings, syndromic-based measures of mortality such as C19P funeral data are not routinely available; however, verbal autopsy provides a well-established retrospective means with which to conduct such inference. Given the scarcity of serological surveys in many settings, such approaches are likely to yield vital data with which to improve our understanding of the future trajectory of the epidemic and the likely impact of different options for control.

C19P funerals and other measures of suspected mortality provide an alternative lens though which to understand the COVID-19 burden but do not allow precise measurement. In the absence of a confirmed diagnosis, the proportion of these individuals who were infected will always be unknown and liable to vary in time and space, as will the extent to which measures of suspected deaths represent all deaths of individuals displaying COVID-19 symptoms. However, irrespective of the data source used, our results highlight the impact of NPIs employed across Java, including substantial COVID-19 associated mortality avoided through swift implementation of control measures in response to the spread of the virus. In particular, our analyses indicate that imposition of stringent measures in Jakarta combined with restrictions on mobility patterns during Ramadan are likely to have delayed the seeding of epidemics to rural, more vulnerable, areas of the island. Given subsequent upwards trends in transmission, this could have potentially accelerated epidemics in such areas beyond currently observed levels. However, current best estimates suggest R_t is now above 1 in all provinces, and our results emphasise the likely worsening of the epidemic across Java. This is consistent with recent observations that healthcare demand in Jakarta is currently heading beyond that observed during the initial peak and threatening to outstrip capacity in the near future (*21*). Our results suggest that the re-imposition of PSBB in Jakarta, beginning on the 14th of September, if successful in suppressing transmission, could largely prevent capacity being exceeded. However, based on current trends, the remaining provinces in Java are likely to be faced with similar choices between re-imposition of suppression measures or exceeded healthcare demand in the coming weeks and months.

Whilst we have attempted to propagate this past uncertainty throughout our analysis of future scenarios, there remain numerous important uncertainties that need to be considered when interpreting these simulations. In particular, both the level of population-level immunity acquired within each scenario (due to factors such as the strength and duration of individual responses) (*31*, *32*) and the level of immunity required to achieve herd immunity are not yet well understood (*30*). However, none of the suppression

scenarios considered here, assuming perfect and durable immunity to reinfection, achieve levels of immunity high enough to preclude a subsequent wave if life were to return to normal and transmissibility were to rise to levels observed at the beginning of the epidemic ($R_t = 2$).

We cannot capture the indirect impact of either suppression measures or that of health systems becoming stretched and/or overwhelmed in this analysis, though both are likely to be high and need to be considered carefully by decision-makers. More broadly, our results highlight that in the short-medium term, levels of population immunity are unlikely to develop to the extent that life in Java can return to pre-pandemic levels of normalcy without leading to substantial incremental increases in mortality. This highlights the need for long-term strategic planning and the urgent need for new tools such as therapeutics and vaccines, even in countries where transmission has not yet been suppressed.

Acknowledgements

This work was supported by Centre funding from the UK Medical Research Council under a concordat with the UK Foreign, Commonwealth and Development Office and the Wellcome Trust, also under a concordat with the UK Foreign, Commonwealth and Development Office. BAD acknowledges a matched MRC Centre 1+3 studentship funding by Imperial College London School of Public Health. IRFE acknowledges a funding from Oxford University Clinical Reseach Unit (OUCRU) Strategic Committee Research for COVID-19, Vietnam. JKB, IRFE, LLE, KDL, RNL, AA, HS are supported by the Wellcome Trust, UK (106680/Z/14/Z). GT is supported by the Wellcome Trust, UK (110179/Z/15/Z). CW acknowledges funding from a UK Medical Research Council Doctoral Training Partnership (DTP) studentship.

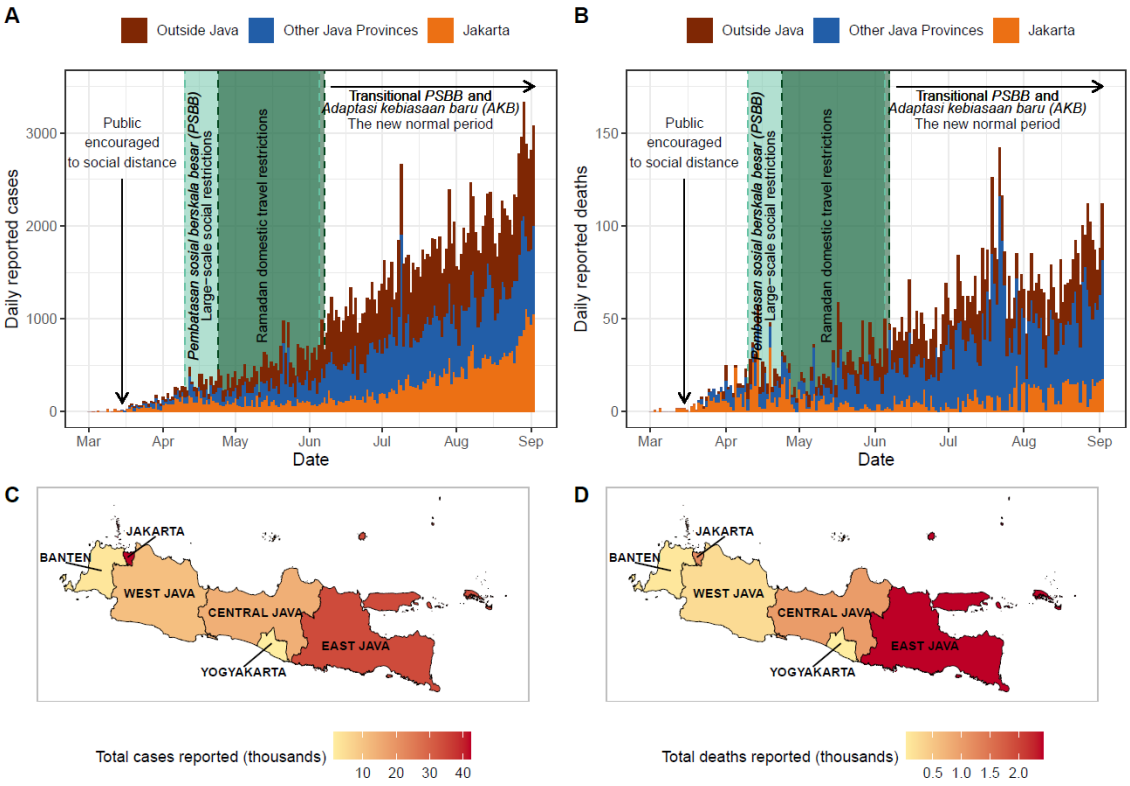

Figure 1. Burden of COVID-19 and timeline of interventions in Indonesia (data up to 2nd September 2020). A) Daily number of reported COVID-19 cases; B) Daily number of reported COVID-19 deaths; C) Total reported COVID-19 cases at province level in Java island; and D) Total reported COVID-19 deaths at province level in Java island.

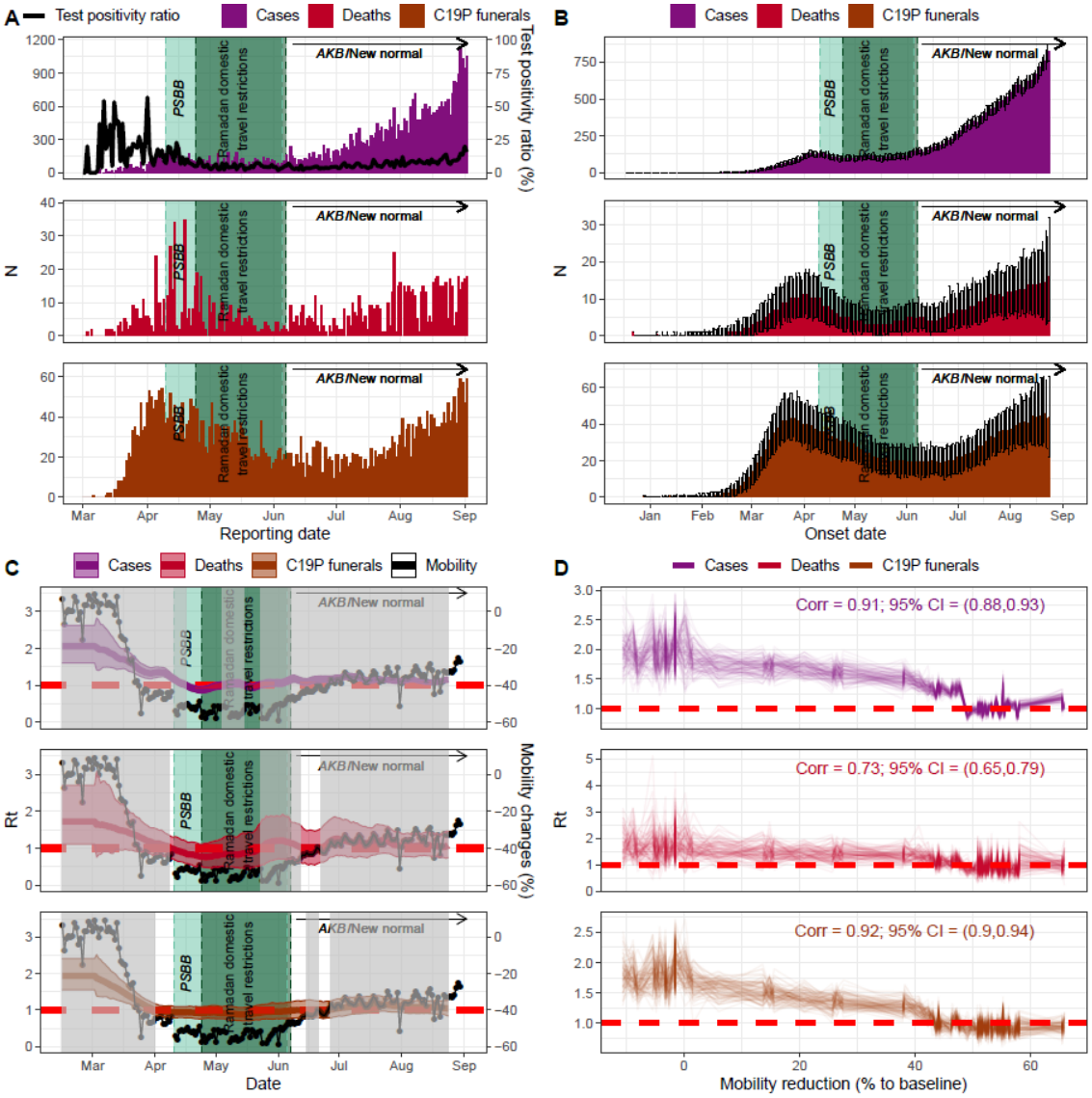

Figure 2. COVID-19-related data, estimated effective reproduction number ( ), and its relationship with the average non-residential mobility changes in Jakarta (epidemiological data up to 2nd September 2020; Google Mobility Reports data up to 30th August 2020). A) Daily reported cases, deaths, and C19P funerals in Jakarta. Black line denotes the daily test positivity ratio; B) Reconstructed daily reported cases, deaths, and C19P funerals to reflect the estimated onset date of each observation; C) Coloured lines and regions show, respectively, median and 95% CrI of estimated (left axis) based on the reconstructed data (cases, deaths or C19P funerals). Grey areas denote periods where the estimated median is above 1. Black lines and dots denote average changes in non-residential mobility (right axis); D) The relationship and correlation coefficient between the estimated and the average non-residential mobility reduction.

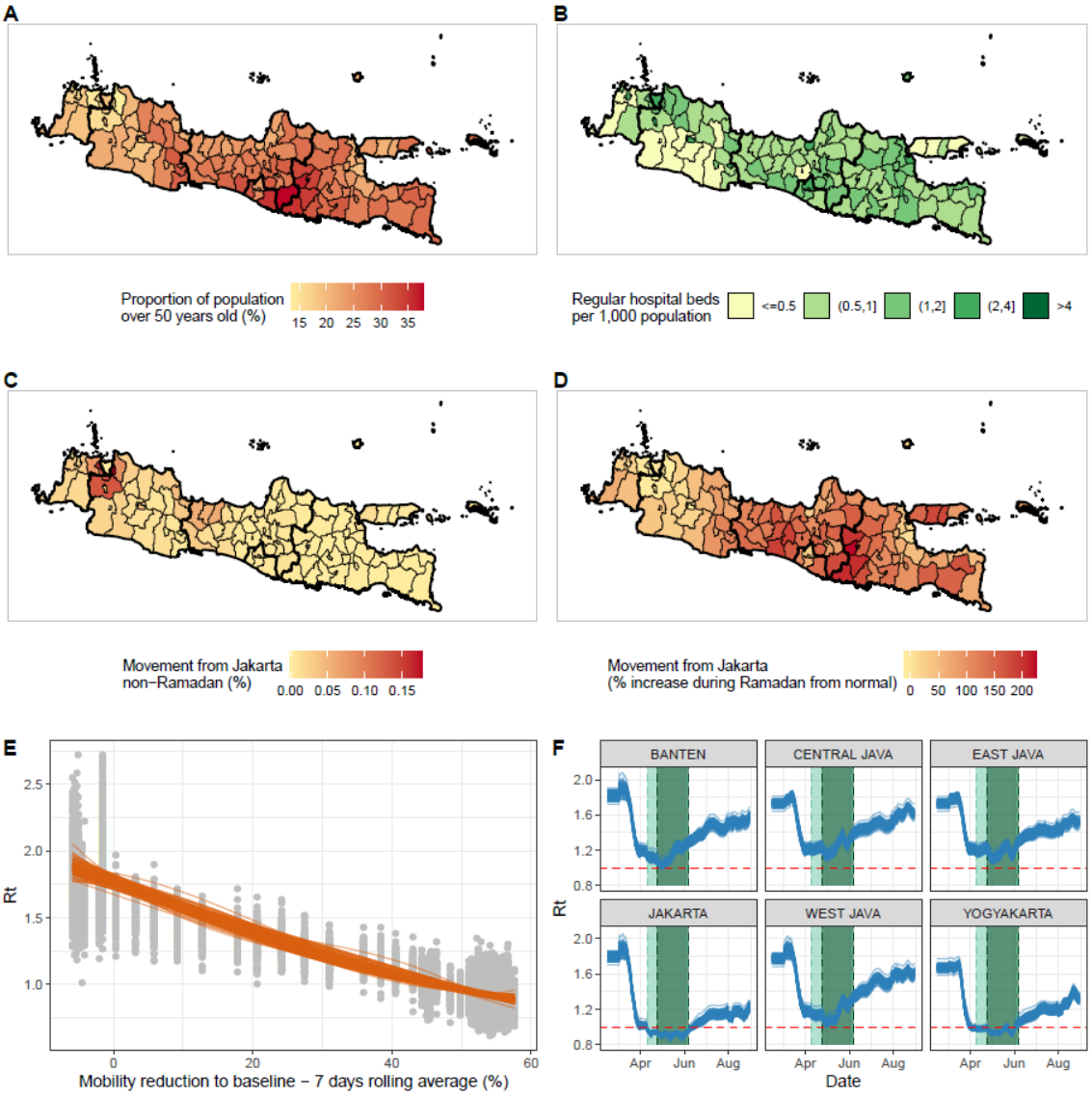

Figure 3. Key factors that are affecting the spread and severity of COVID-19 epidemic in Java, Indonesia. A) Proportion of the population aged over 50 years old at the district level; B) Number of regular hospital beds per one thousand population at the district level; C) Proportion of Jakarta residents who spent their day in other districts in Java during a non-Ramadan period; D) Increased proportion of people of Jakarta who spent their day in other districts in Java during Ramadan compared to the non-Ramadan period; E) The relationship between the estimated values based on C19P funerals data and average reduction in non-residential mobility in Jakarta. Orange lines show the modelled smoothing spline relationship for 100 samples; and F) Extrapolations of values in provinces in Java based upon Google Mobility trends for each province and the 100 sampled smoothing splines in E.

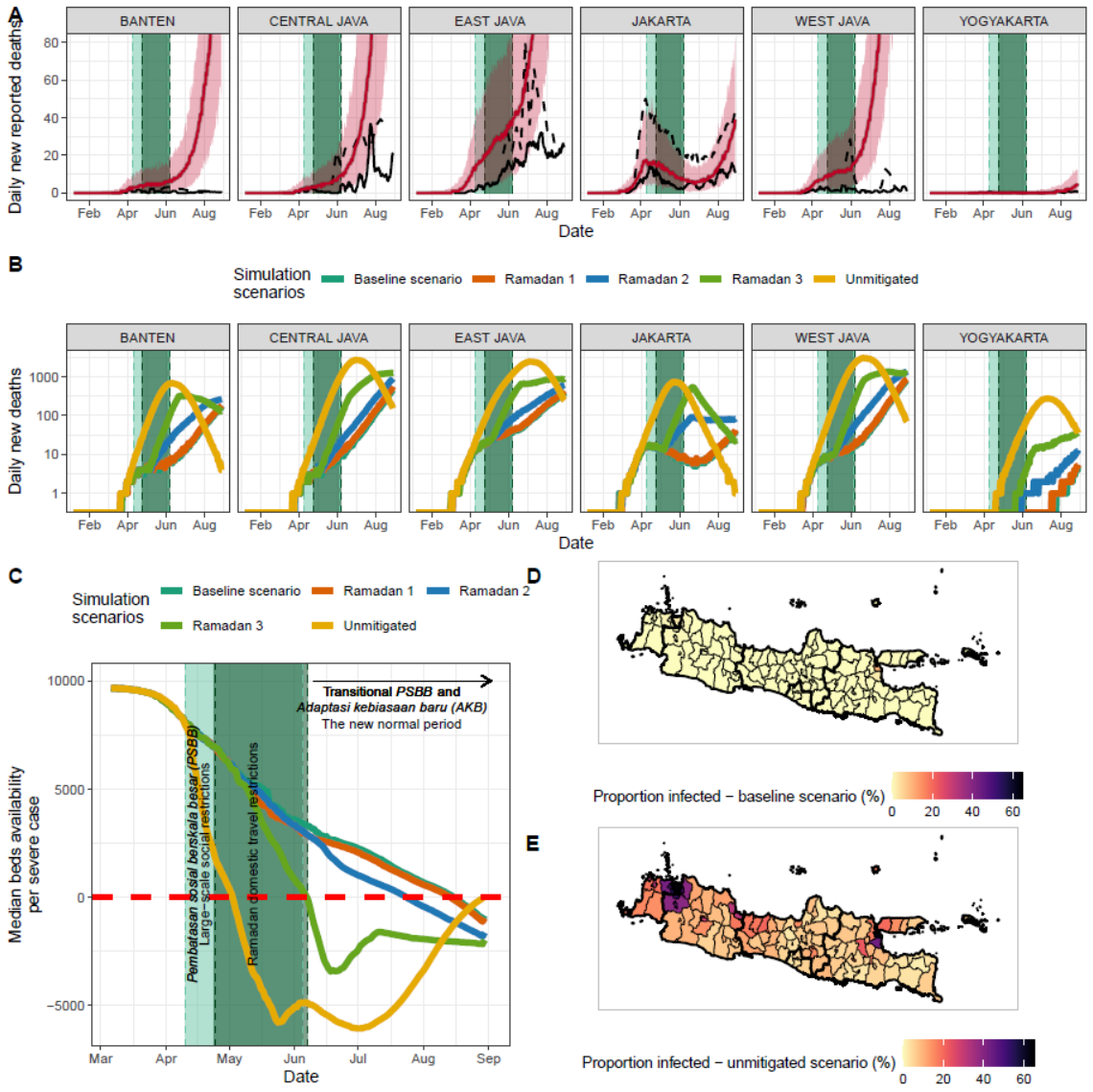

Figure 4. Metapopulation model simulation results. A) Comparison of model simulations (red lines and their shaded 95% uncertainties ranges) and daily confirmed (solid black lines) and suspected (dashed black lines) deaths from COVID-19; B) Model simulations in five different scenarios: 1) Baseline scenario as shown in A, 2) Ramadan counter-factual 1 where it is assumed that there is no movement restrictions during the Ramadan period and values are similar to the baseline scenario, 3) Ramadan counter-factual 2 where it is assumed that there is no movement restrictions during the Ramadan period and values are 75% of each district's value, 4) Ramadan counter-factual 3 where it is assumed that there are no movement restrictions during the Ramadan period and values are each district's value and 5) Unmitigated scenario where no interventions since the beginning of the epidemic are assumed; C) Median hospital beds availability per severe COVID-19 case over time based on different simulation scenarios; D) Proportion of people infected based on the actual scenario up to 31st May 2020 (before AKB/the 'new normal') at the district level; and E) Proportions of people infected based on the unmitigated scenario up to 31st May 2020 (before AKB) at the district level.

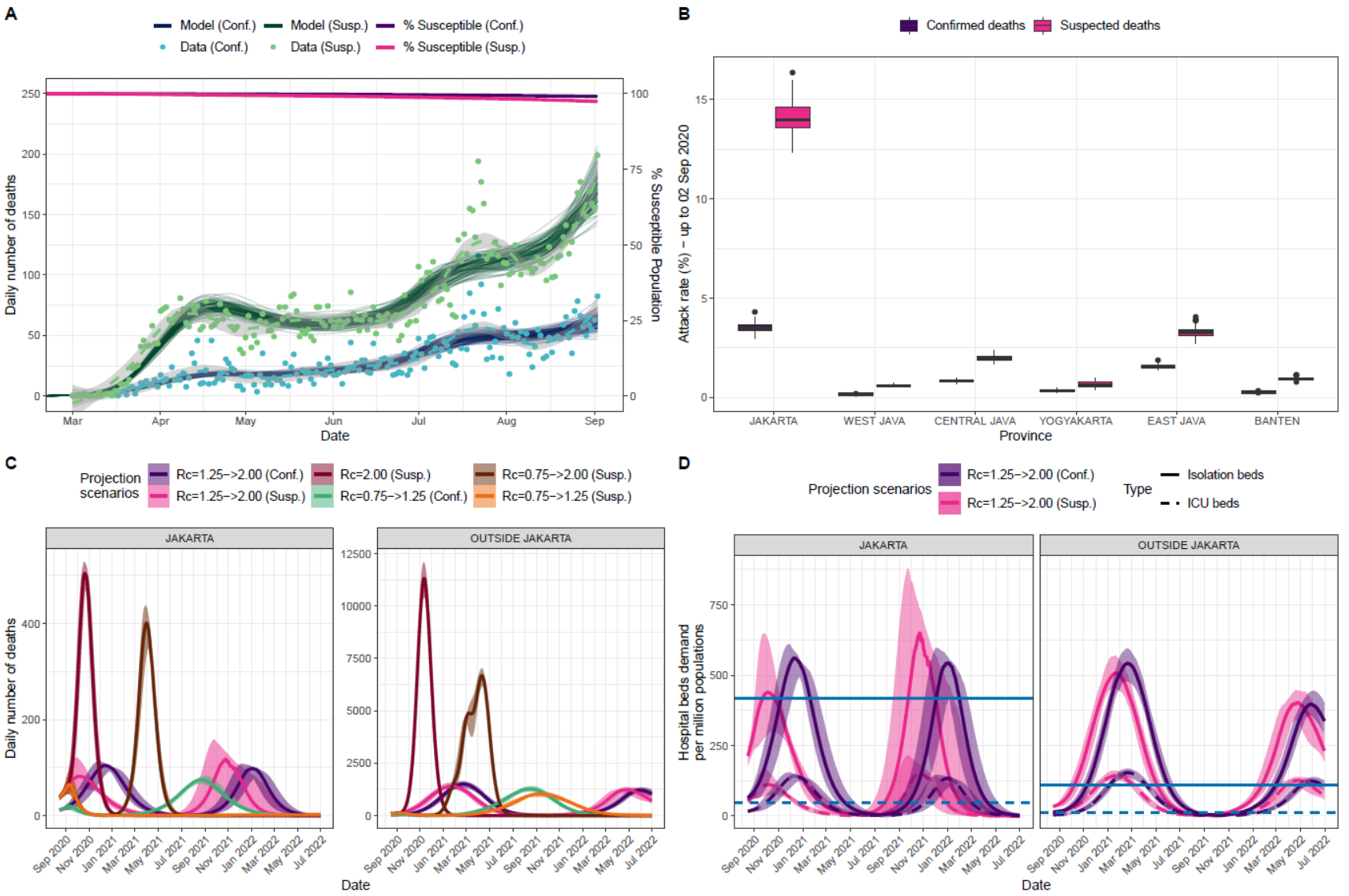

Figure 5. A) Model fitting to confirmed and suspected (both confirmed and probable) COVID-19 related deaths and inferred population susceptibility in Java; Green and blue dots show data on reported and suspected respectively (where suspected includes augmented estimate of probably deaths in provinces outside Jakarta pre-May 13th), with associated median (lines) and 95% CrI (shaded areas) of model fits. B) Estimated province-level attack rates (cumulative proportion infected) based on confirmed (purple) and suspected COVID-19 related deaths; C) Projections of daily number of deaths due to COVID-19 based on four different transmissibility scenarios; and D) Healthcare demand projections in the form of isolation beds and ICU beds demands assuming the current level of transmission to continue in the future (with easing of control measures after the transmission reached a low-level following the first peak in the graph). Projections are coloured according to whether they are based upon confirmed or suspected deaths to date and by projected R_c (with $R_c = x -> y$ representing $R_c = x$ for immediate future and $R_c = \mathrm{y}$, the level it returns to when burden falls below 7 deaths per week). Healthcare capacities are based on the current numbers of dedicated COVID-19 isolation beds and ICUs (*33*), not reflecting the total number of beds and ICUs in each province.

Table 1. Total number of estimated deaths based on model simulations of the actual epidemic scenario and its counterfactual of an unmitigated scenario (assuming no interventions) from the beginning of the epidemic up to 31st May. Values inside the brackets denote 95 percentile range of simulations. Suspected deaths are a combination of confirmed and probable COVID-19 deaths.

Province	Confirmed deaths 13th-31st May (WHO Indonesia situation report 10 (*18*))	Suspected deaths 13th-31st May (WHO Indonesia situation report 10 (*18*))	Baseline model scenario deaths 13th-31st May	Confirmed deaths up to 31st May ((*14*, *22*))	Suspected deaths up to 31st May (provincial data collated by KawalCOVID19 (*29*))	Baseline model scenario deaths up to 31st May	Unmitigated counterfactual deaths up to 31st May	Averted deaths up to 31st May (unmitigated – baseline)
Jakarta	74	447	192 (76-455)	520	2,435	960 (356-2,331)	20,332 (11,447-29,299)	19,382 (11,011-27,002)
West Java	46	351	230 (79-566)	135	653	621 (236-1,502)	21,025 (9,165-49,866)	20,489 (8,816-48,379)
Central Java	4	269	114 (30-316)	66	666	262 (89-694)	7,736 (3,106-19,205)	7,480 (3,004-18,441)
Yogyakarta	0	1	2 (0-8)	9	29	8 (2-32)	493 (162-1,282)	487 (158-1,251)
East Java	241	458	574 (166-1,279)	395	1,127	1,441 (413-3,521)	15,170 (5,472-30,061)	13,461 (5,066-27,045)
Banten	13	47	87 (29-231)	67	332	269 (76-655)	8,352 (2,960-18,489)	8,059 (2,858-17,840)
Java island total	378	1,638	1,260 (493-2,524)	1,192	5,242	3,696 (1,488-7,379)	74,994 (36,355-142,749)	71,250 (34,400-136,001)

References

1. World Health Organization (WHO), Novel Coronavirus – China (2020), (available at https://www.who.int/csr/don/12-january-2020-novel-coronavirus-china/en/).

2. WHO, WHO Coronavirus Disease (COVID-19) Dashboard (2020), (available at https://covid19.who.int/).

3. K. Mizumoto, K. Kagaya, A. Zarebski, G. Chowell, Estimating the asymptomatic proportion of coronavirus disease 2019 (COVID-19) cases on board the Diamond Princess cruise ship, Yokohama, Japan, 2020. *Eurosurveillance*. **25**, 2000180 (2020).

4. O. J. Watson, M. Alhaffar, Z. Mehchy, C. Whittaker, Z. Akil, Imperial College London COVID-19 Response Team, F. Checchi, N. Ferguson, A. Ghani, E. Beals, P. Walker, A. Authors*, "Report 31: Estimating the burden of COVID-19 in Damascus, Syria: an analysis of novel data sources to infer mortality under-ascertainment" (Imperial College London, 2020).

5. T. Burki, COVID-19 in Latin America. *Lancet Infect. Dis.* **20**, 547–548 (2020).

6. S. Flaxman, S. Mishra, A. Gandy, H. J. T. Unwin, T. A. Mellan, H. Coupland, C. Whittaker, H. Zhu, T. Berah, J. W. Eaton, M. Monod, P. N. Perez-Guzman, N. Schmit, L. Cilloni, K. E. C. C. Ainslie, M. Baguelin, A. Boonyasiri, O. Boyd, L. Cattarino, L. V. Cooper, Z. Cucunubá, G. Cuomo-Dannenburg, A. Dighe, B. Djaafara, I. Dorigatti, S. L. van Elsland, R. G. FitzJohn, K. A. M. M. Gaythorpe, L. Geidelberg, N. C. Grassly, W. D. Green, T. Hallett, A. Hamlet, W. Hinsley, B. Jeffrey, E. Knock, D. J. Laydon, G. Nedjati-Gilani, P. Nouvellet, K. V. Parag, I. Siveroni, H. A. Thompson, R. Verity, E. Volz, C. E. Walters, H. Wang, Y. Wang, O. J. Watson, P. Winskill, X. Xi, P. G. Walker, A. C. Ghani, C. A. Donnelly, S. M. Riley, M. A. C. C. Vollmer, N. M. Ferguson, L. C. Okell, S. Bhatt, Estimating the effects of non-pharmaceutical interventions on COVID-19 in Europe. *Nature*. **584**, 257–261 (2020).

7. D. Spiegelhalter, Why has the UK done so badly on Covid-19? There are still no simple answers. *Guard.* (2020), (available at https://www.theguardian.com/commentisfree/2020/aug/02/uk-covid-19-excess-deaths).

8. T. Cocks, How inequality and poverty undermined South Africa's COVID response. *Reuters* (2020), (available at https://www.reuters.com/article/us-health-coronavirus-safrica-response-a-idUSKCN24W1OL).

9. C. Nugent, How Peru's Coronavirus Outbreak Got So Bad: What to Know. *Time* (2020), (available at https://time.com/5844768/peru-coronavirus/).

10. "No coffins or oxygen": Bolivia struggling amid coronavirus surge. *Al Jazeera* (2020), (available at https://www.aljazeera.com/news/2020/07/coffins-oxygen-bolivia-struggling-coronavirus-surge-200724081503555.html).

11. United Nations Office for the Coordination of Humanitarian Affairs (UN OCHA) Syria, WHO Syria, Syrian Arab Republic: COVID-19 Update No. 16 (2020), (available at https://reliefweb.int/report/syrian-arab-republic/syrian-arab-republic-covid-19-update-no-16-16-august-2020).

12. E. Akinwotu, M. Hodi, 'We depend on God': gravediggers on frontline of Kano's Covid-19 outbreak. *Guard.* (2020), (available at https://www.theguardian.com/global-

development/2020/may/11/we-depend-on-god-gravediggers-on-frontline-of-kanos-covid-19-outbreak).

13. M. A. Benítez, C. Velasco, A. R. Sequeira, J. Henríquez, F. M. Menezes, F. Paolucci, Responses to COVID-19 in five Latin American countries. *Heal. policy Technol.*, 449 (2020).

14. Satuan Tugas Penanganan COVID-19 (Indonesia COVID-19 Response Acceleration Task Force), Peta Sebaran (2020), (available at https://covid19.go.id/peta-sebaran).

15. D. Rochmyaningsih, Indonesia finally reports two coronavirus cases. Scientists worry it has many more. *Science (80-.).* (2020), doi:10.1126/science.abb5653.

16. P. M. De Salazar, R. Niehus, A. Taylor, C. O. F. Buckee, M. Lipsitch, Identifying Locations with Possible Undetected Imported Severe Acute Respiratory Syndrome Coronavirus 2 Cases by Using Importation Predictions. *Emerg. Infect. Dis.* **26**, 1465–1469 (2020).

17. M. I. Gorbiano, BREAKING: Jokowi announces Indonesia's first two confirmed COVID-19 cases (2020), (available at https://www.thejakartapost.com/news/2020/03/02/breaking-jokowi-announces-indonesias-first-two-confirmed-covid-19-cases.html).

18. WHO Indonesia, COVID-19 Indonesia Situation Reports (2020), (available at https://www.who.int/indonesia/news/novel-coronavirus/situation-reports).

19. This year's Idul Fitri traffic accidents fall by 31 percent. *Jakarta Post* (2020), (available at https://www.thejakartapost.com/news/2020/06/09/this-years-idul-fitri-traffic-accidents-fall-by-31-percent.html).

20. B. Sutrisno, "Transitional PSBB": A deciding chapter for Jakarta's new normal. *Jakarta Post* (2020), (available at https://www.thejakartapost.com/news/2020/06/09/transitional-psbb-a-deciding-chapter-for-jakartas-new-normal.html).

21. S. Widianto, Indonesia's capital to reimpose restrictions over coronavirus. *Reuters* (2020), (available at https://uk.reuters.com/article/health-coronavirus-indonesia-idINL4N2G62U5).

22. Jakarta Provincial Health Department, Jakarta COVID-19 Data Monitoring (2020), (available at https://corona.jakarta.go.id/id/data-pemantauan).

23. R. Verity, L. C. Okell, I. Dorigatti, P. Winskill, C. Whittaker, N. Imai, G. Cuomo-Dannenburg, H. Thompson, P. G. T. T. Walker, H. Fu, A. Dighe, J. T. Griffin, M. Baguelin, S. Bhatia, A. Boonyasiri, A. Cori, Z. Cucunubá, R. FitzJohn, K. Gaythorpe, W. Green, A. Hamlet, W. Hinsley, D. Laydon, G. Nedjati-Gilani, S. Riley, S. van Elsland, E. Volz, H. Wang, Y. Wang, X. Xi, C. A. Donnelly, A. C. Ghani, N. M. Ferguson, Estimates of the severity of coronavirus disease 2019: a model-based analysis. *Lancet Infect. Dis.* **20**, 669–677 (2020).

24. A. Cori, N. M. Ferguson, C. Fraser, S. Cauchemez, A new framework and software to estimate time-varying reproduction numbers during epidemics. *Am. J. Epidemiol.* **178**, 1505–12 (2013).

25. Google LLC, Google COVID-19 Community Mobility Reports, (available at

https://www.google.com/covid19/mobility/).

26. K. E. C. Ainslie, C. E. Walters, H. Fu, S. Bhatia, H. Wang, X. Xi, M. Baguelin, S. Bhatt, A. Boonyasiri, O. Boyd, L. Cattarino, C. Ciavarella, Z. Cucunuba, G. Cuomo-Dannenburg, A. Dighe, I. Dorigatti, S. L. van Elsland, R. FitzJohn, K. Gaythorpe, A. C. Ghani, W. Green, A. Hamlet, W. Hinsley, N. Imai, D. Jorgensen, E. Knock, D. Laydon, G. Nedjati-Gilani, L. C. Okell, I. Siveroni, H. A. Thompson, H. J. T. Unwin, R. Verity, M. Vollmer, P. G. T. T. Walker, Y. Wang, O. J. Watson, C. Whittaker, P. Winskill, C. A. Donnelly, N. M. Ferguson, S. Riley, Evidence of initial success for China exiting COVID-19 social distancing policy after achieving containment. *Wellcome Open Res.* **5**, 81 (2020).

27. P. Nouvellet, S. Bhatia, A. Cori, Imperial College London COVID-19 Response Team, N. Ferguson, C. A. Donnelly, “Report 26: Reduction in mobility and COVID-19 transmission” (Imperial College London, 2020).

28. P. G. T. Walker, C. Whittaker, O. J. Watson, M. Baguelin, P. Winskill, A. Hamlet, B. A. Djafaara, Z. Cucunubá, D. Olivera Mesa, W. Green, H. Thompson, S. Nayagam, K. E. C. Ainslie, S. Bhatia, S. Bhatt, A. Boonyasiri, O. Boyd, N. F. Brazeau, L. Cattarino, G. Cuomo-Dannenburg, A. Dighe, C. A. Donnelly, I. Dorigatti, S. L. van Elsland, R. FitzJohn, H. Fu, K. A. M. M. Gaythorpe, L. Geidelberg, N. Grassly, D. Haw, S. Hayes, W. Hinsley, N. Imai, D. Jorgensen, E. Knock, D. Laydon, S. Mishra, G. Nedjati-Gilani, L. C. Okell, H. J. Unwin, R. Verity, M. Vollmer, C. E. Walters, H. Wang, Y. Wang, X. Xi, D. G. Lalloo, N. M. Ferguson, A. C. Ghani, The impact of COVID-19 and strategies for mitigation and suppression in low- and middle-income countries. *Science (80-.).* **369**, eabc0035 (2020).

29. COVID-19 di Indonesia @kawalcovid19 online spreadsheet (tab: Kasus per Provinsi) (2020), (available at kcov.id/daftarpositif).

30. T. Britton, F. Ball, P. Trapman, A mathematical model reveals the influence of population heterogeneity on herd immunity to SARS-CoV-2. *Science (80-.).* **369**, 846–849 (2020).

31. D. M. Altmann, D. C. Douek, R. J. Boyton, What policy makers need to know about COVID-19 protective immunity. *Lancet*. **395**, 1527–1529 (2020).

32. D. S. Stephens, M. J. McElrath, COVID-19 and the Path to Immunity. *J. Am. Med. Assoc.* (2020), , doi:10.1001/jama.2020.16656.

33. Ministry of Health of the Republic of Indonesia, “Ketahanan Kesehatan dalam Menjalani Tatanan Hidup Baru” (Jakarta, 2020).

Supplementary Material

Materials and Methods

S1. Data Sources and Curation

Epidemiological data sources for Jakarta

Epidemiological data for Jakarta were obtained from the official Jakarta COVID-19 data monitoring website (https://corona.jakarta.go.id/id/data-pemantauan) (*1*). This data comprises daily reported cases, reported deaths, funerals with COVID-19 protocol (C19P), and the number of tests. We collate the data for analysis up to 2nd September 2020.

Anonymous individual data of 11,280 confirmed COVID-19 cases up to 29th June 2019 in Jakarta were obtained from the Jakarta Department of Health. Data consist of dates of onset of symptoms, dates of attendance in the hospital, and dates of deaths. The individual data were used to estimate the delay distributions between onset to diagnosis and onset to death.

Epidemiological data sources for five other provinces in Java (Banten, West Java, Central Java, Yogyakarta, and East Java)

Daily reported cases and reported deaths data for five other provinces in Java were obtained from an independently curated online spreadsheet by a crowdsource organisation KawalCOVID19 (kcov.id/daftarpositif) (*2*) based on the daily publication by Indonesia COVID-19 National Task Force (*3*) (data for analysis were collated up 2nd September 2020). The weekly number of deaths of suspected and probable cases was obtained from WHO Indonesia situation reports 13-23 (*4*).

Call detail records data

Anonymised call detail records (CDRs) data from one of the biggest telecommunication companies in Indonesia over the period of 1st May 2011 to 30th April 2012 were used to estimate between-district movement matrices for the Ramadan and non-Ramadan period. The CDRs data were collected daily with a total of 266 billion records and 137 million unique SIM cards. There were a total of 17,319 mobile phone towers operated during the period of CDRs data collection across the country.

Province-level mobility changes

Province-level mobility changes data were acquired from the freely-available Google COVID-19 Community Mobility Reports (https://www.google.com/covid19/mobility/) (*5*). Google Mobility Reports data up to 30th of August 2020 were used for the analysis.

Healthcare capacity data

District-level hospital and ICU beds data were obtained from the Online Healthcare Facilities (*Fasyankes Online*) website by the Directorate General of Health Services (*Ditjen Yankes*) of the Ministry of Health of the Republic of Indonesia (*6*).

Dedicated COVID-19 isolation beds and ICU beds data

Data for the capacity of dedicated COVID-19 isolation beds and ICU beds were obtained from a report from the Ministry of Health in August 2020 (*7*).

S2. Epidemiological Data Reconstructions

Daily reported cases, reported deaths, and C19P funerals data in Jakarta were reconstructed to represent the onset day of each reported event using estimates of the distribution of delays between onset and diagnosis and onset and death. Each C19P funeral was assumed to occur the day following the date of death.

The distributions of onset to diagnosis and onset to death of confirmed COVID-19 cases were estimated by fitting discretised Gamma distributions (*8*) to the individual patient data obtained from the Jakarta Department of Health (**Fig S1**). The mean estimate of the onset to diagnosis delay was 7.62 days, with a standard deviation of 7.51 days. The mean estimate of the onset to death delay was 15.87 days, with a standard deviation of 9.34 days. 100 sets of reconstructed daily frequencies of onset of cases, deaths, and funerals were then calculated on the basis of 100 draws for each reported event from these distributions (respectively onset to hospitalisation, onset to death, and onset to funeral). Adjustment for right censoring occurring due to individuals currently with symptoms but have yet to reach outcome was carried out by dividing the inferred onset frequency on a given day by the cumulative probability it would have been observed by the last date within the dataset.

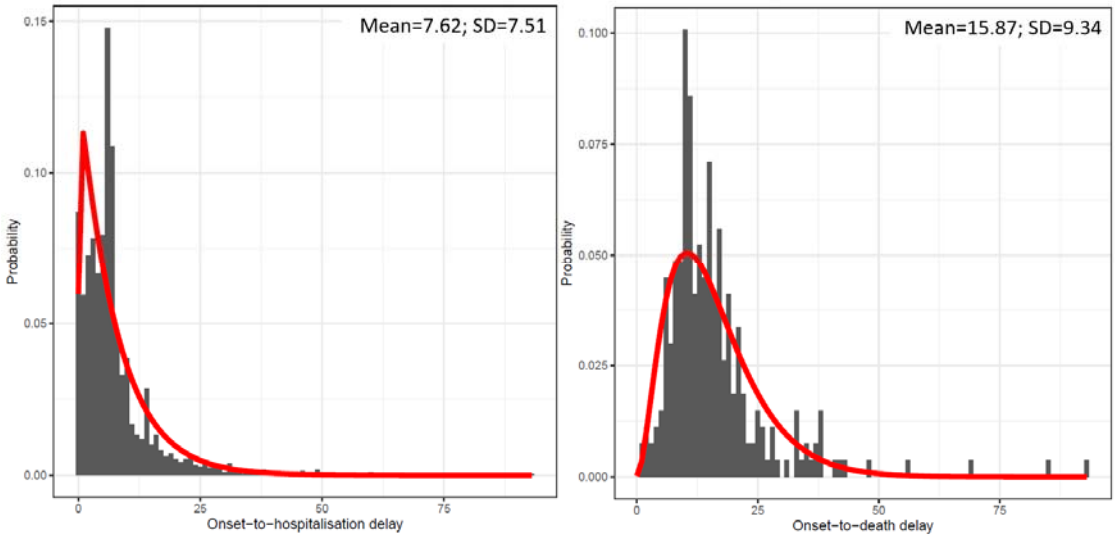

Supplementary Figure S1: Discretised Gamma distribution fittings to onset-to-hospitalisation delay data (left) and onset-to-death delay data (right).

S3. Effective reproduction number ( ) calculations based on reconstructed epidemiological data in Jakarta and its relationship with daily mobility changes

The daily effective reproduction number in Jakarta was estimated using the EpiEstim R package (*9*, *10*) for each reconstructed cases ( ), deaths ( ), funerals ( ) data. at the

beginning of the epidemic was estimated for the period before 2nd March 2020 (the day where the country's first two cases were announced). Subsequently, R_t was estimated over a weekly sliding window, with a mean and standard deviation of serial interval distribution were assumed to be 6.3 and 4.2 days, respectively (*11*).

1,000 random samples were drawn from the posterior samples of the estimated $R_{t,cases}$, $R_{t,deaths}$, and $R_{t,funerals}$ at each timepoint. Pearson's correlation coefficients for estimates based on cases, deaths, and funerals data were calculated against the daily average changes in non-residential mobility in Jakarta based on Google mobility estimates. The daily average changes in non-residential mobility is the average of changes of retail and recreation, grocery and pharmacy, parks, transit stations, and workplaces types of mobility to each respective baseline.

The 7-day rolling average changes of non-residential mobility were fitted to 100 posterior samples of the estimated $R_{t,funerals}$ using smoothing spline models. The implementation of the smoothing spline model was done in R software using *smooth.spline* function with four knots. The models were then used to extrapolate the daily values of R_t outside of Jakarta based on the province-level 7-day rolling average of changes in non-residential mobility (Google Community Mobility Reports (*5*)).

S4. Estimating movement matrices from CDRs data

District level (city and municipality, 115 in total) movement matrices (M) prior to the pandemic for the normal (or non-Ramadan) (M_N) and Ramadan (M_R) periods were calculated from CDRs data. Each element of the matrix ($m_{i,j}$) represents the proportion of days spent by residents of district i in district j over the year.

The daily position of each user is described as the district where the most frequent mobile phone usage happened over the period of a single day. All users were assumed to be active from the first day to the last day of their phone usage. On days where the user was not active (no phone activities recorded), the position of the user was assumed to be the same as the previous day. The primary residence of each user is defined as the district where the users spent most of their days over their 'active' period. Based on their daily locations and primary residences, we then calculated the proportion of days spent of people from district i in district j. M_R was estimated using data of August and September 2011 (period of the Ramadan month, Eid celebration, and national holidays period). M_N was estimated using the rest of the data that were not used to estimate M_R (May 2011 - July 2011 and October 2011 - April 2012 periods).

All districts in the Java island were represented as a single row in each matrix with exceptions for districts in Jakarta province which were represented as an aggregated single row of Jakarta 'megacity'. Outside Java movements were represented as a single row ($i = 2$). **Table S2** shows a complete list of districts (including Jakarta and outside Java) and each respective index in the movement matrix.

S6. Metapopulation Model

Metapopulation model of COVID-19 spread in Java

We developed a metapopulation model to simulate the spread of COVID-19 in Java. Each patch in the metapopulation model represents districts ($i = 1,2,\ldots,115$) listed in **Table S2**. For each patch,

stochastic differential equations representing a Susceptible-Exposed-Infected-Recovered (SEIR) model were implemented (overall structure in **Figure S2**). The equations are as follows:

$$\frac{dS_i}{dt} = -new\ infections_i$$

$$\frac{dE_i}{dt} = new\ infections_i - \alpha E_i$$

$$\frac{dI_{mild,i}}{dt} = (1 - p_{hosp,i})\ \alpha E_i - \gamma_1 I_{mild,i}$$

$$\frac{dI_{case,i}}{dt} = p_{hosp,i}\ \alpha E_i - \gamma_2 I_{case,i}$$

$$\frac{dR_i}{dt} = \gamma_1 I_{mild,i} + \gamma_2 I_{case,i}$$

where $new\ infections_i$ is the number of new infections in each patch based on the stochastic adaptation of the metapopulation transmission model by Keeling et al. (*12*). To calculate $new\ infections_i$, we firstly need to calculate the district-level force of infections λ_i that accounts for inter-district movements of both susceptible individuals (that might acquire infections in other districts) and infected individuals (that might infect people in other districts) based on the inter-patch connectivities (the movement matrix, M, accounting daily changes in mobility - see **section S4**). The total number of infected individuals that are contributing to infections in district i, $I_{tot,i}$, is calculated by:

$$I_{tot,i} = \sum_{j=1}^{115} Binomial(I_j, m_{j,i}).$$

The transmission rate for each district is calculated by:

$$\beta_i = \frac{R_{0,i}}{((1-p_{hosp,i})\gamma_1 + p_{hosp,i}\gamma_2)},$$

where $R_{0,i}$ is the value of R_t estimated for the period of maximum mobility recorded within Google Mobility data.

Hence,:

$$\lambda_i = \beta_i \times \kappa_{t,i} \times \frac{I_{tot,i}}{N_i},$$

where N_i is the total population of each district/patch and $\kappa_{t,i}$ is the daily ratio between the estimated $R_{t,i}$ values based on the spline model estimates and the respective $R_{0,i}$, representing the relative changes in the daily transmission rate. We assumed no transmission contributed to and from outside Java but we still allow movement to and from that patch ($i = 2$) which implies both I_2 and λ_2 are always 0.

$new\ infections_i$ are then calculated as:

$$new\ infections_i = \sum_{j=1}^{115} Binomial(S_i \times m_{i,j}, (1 - exp(-\lambda_j)))$$

For each severe infection needing hospitalisation (I_{case}), the case was either deemed a critical case (i.e., indicated to require an ICU bed) with probability $p_{critical|hosp}$ and otherwise non-critical (i.e., indicated to require an isolation bed) with associated probability of death ($p_{death|non\ critical}$ and $p_{death|critical}$). p_{hosp}, $p_{critical|hosp}$, $p_{death|non\ critical}$ and $p_{death|critical}$ were obtained for each district as the average values estimated within simulations from the squire package (*13*), taking age-specific demography using district-level census data and, in the absence of equivalent data from Java, mixing patterns based upon a contact survey from Shanghai province, China as an example of contact patterns within a UMIC Asian country and province containing a megacity. The full model parameter descriptions and specifications are available in **Table S1**.

The model was simulated with 100 replicates by seeding initial cases in Jakarta, and Kota Surabaya (East Java's capital) – both have international airports receiving travellers from China – on 7th January 2020 (arbitrarily selected) with 100 replicates. Initial cases in Jakarta were set to 12, obtained through calibration to provide simulated deaths trends bounded by the interval between reported deaths and C19P funerals. Initial cases in Surabaya were drawn according to a binomial draw assuming an underlying importation rate of 60% of that in Jakarta (*14*), random numbers based on the binomial distribution were sampled for each replicate.

We assumed different transmission scenarios of districts classified as rural and urban districts. We classified an urban/rural status to each district based upon the urban/rural classification of the majority of villages within the district. We assigned $R_{t,i}$ values for all districts to be the province-level value of $R_{t,i}$ in which each district is located. We then explore the possibilities of rural districts to have different $R_{t,i}$ levels, ranging from 100% to 60% of province-level $R_{t,i}$. In the results section of the main text, we show simulation results assuming $R_{t,i}$ in rural districts to be 90% of $R_{t,i}$ in urban districts. We also ran the model for several different counterfactual scenarios. The list of transmission scenarios and the counterfactual scenarios were shown in **Table S3**.

During the period of Ramadan and Eid festivals, 24th April 2020 up to 7th June 2020, the Ramadan movement matrix (M_R) was used as the baseline movement matrix. In the other period, the non-Ramadan movement matrix (M_N) was used as the baseline movement matrix. As a baseline assumption, throughout the simulation, the proportions of people spending their time in other districts ($m_{i,j}$ where $i \neq j$) were adjusted by the province-level changes in mobility over time, with reductions in larger-scale movement outside the province assumed to be higher than those within the province according to an odds ratio (OR) of 2 within our default scenario.

For each scenario, we also devised a metric to assess the extent to which the epidemic would be likely to strain available healthcare resources over time given patterns of spatial spread and disparities in healthcare supply by district. This metric was defined by determining the number of available beds for each individual newly requiring hospitalisation each day within the model by subtracting the number of hospital beds required in the simulation from the total hospital beds capacity available at the district-level obtained from the Online Healthcare Facilities website (*6*).

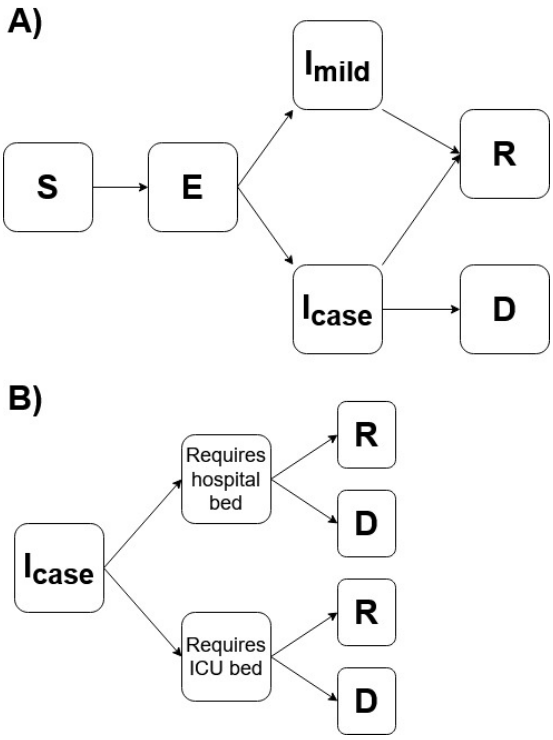

Supplementary Figure S2: SEIR model structure. A) The SEIR structure for each patch in the metapopulation model. Susceptible individuals ($\boldsymbol{S}$), if infected, progress to the exposed compartment ($\boldsymbol{E}$), having their latent period of infections. Then, those individuals will either develop mild symptoms ($\boldsymbol{I_{mild}}$) or severe symptoms requiring hospitalisations (I_{case}). Those who developed severe symptoms may have two possible outcomes: recovery (R) or death (D); **B)** The pathway of infections requiring hospitalisations (I_{case}). Each infection with severe symptoms may only need a standard hospital bed or may develop worse conditions that require critical care (ICU bed). Each of those cases treated in both critical and non-critical care may recover or die based on specific probabilities.

Supplementary Table S1: Model parameters descriptions and values for the metapopulation model.

Parameter	Symbol	Value	Description
Transmission rate	β_i	-	Calculated from $R_{0,i}$.
Basic reproduction number	$R_{0,i}$	-	Estimated from the maximum values of the smoothing spline models between mobility changes and $R_{t,funerals}$.
Relative changes in daily transmission rate	κ_i	-	The ratio between $R_{0,i}$ and daily estimated $R_{t,i}$ based on spline smoothing models.

Mean latent period	$1/\alpha$	4.6 days	Estimated as 5.1 days (*15*) with 0.5 days accounted as a pre-symptomatic period of infectiousness.
Mean duration of infectiousness of mild infections	$1/\gamma_1$	2.1 days	0.5 days infectiousness period prior to symptoms included which in combination with mean duration of severe illness gives a mean serial interval of 6.75 days (*11*).
Mean duration of infectiousness of severe infections	$1/\gamma_2$	4.5 days	Mean onset to admission to hospital of 4 days, as used in squire model (*16*), based on unpublished analysis of data from the ICNARC study (*17*) and includes 0.4 days of infectiousness prior to symptoms.
Probability of having severe illness, needing hospitalisations	$p_{hosp,i}$	**Table S2**	For each district, the probability was calculated by running a full unmitigated epidemic in squire package (*13*). The proportion of people needing hospitalisations were calculated based on the simulations.
Probability of needing critical care, if hospitalised	$p_{critical\|hosp,i}$	**Table S2**	For each district, the probability was calculated by running a full unmitigated epidemic in squire package (*13*). The proportion of people needing hospitalisations were calculated based on the simulations.
Probability of death of severe illness that does not need critical care	$p_{death\|non\ critical,i}$	**Table S2**	For each district, the probability was calculated by running a full unmitigated epidemic in squire package (*13*). The proportion of people needing hospitalisations were calculated based on the simulations.
Probability of death of severe illness that needs critical care	$p_{death\|critical,i}$	0.5	Probability of death from severe illness needing critical care based on the data of the ICNARC study in the UK (*17*).

Supplementary Table S2: List of districts, districts' indexes, and probability of disease severity and outcomes for the metapopulation model.

Index no.	District	Province	$p_{hosp,i}$	$p_{\substack{critical\mid \\ hosp,i}}$	$p_{\substack{death\mid \\ non\ critical,i}}$
1	Jakarta	Jakarta	0.029	0.185	0.054
2	Outside Java	Outside Java	0.027	0.195	0.058
3	Bogor	West Java	0.026	0.190	0.056
4	Sukabumi	West Java	0.031	0.216	0.065
5	Cianjur	West Java	0.031	0.212	0.064
6	Bandung	West Java	0.028	0.201	0.060
7	Garut	West Java	0.030	0.219	0.067
8	Tasikmalaya	West Java	0.034	0.228	0.070
9	Ciamis	West Java	0.039	0.234	0.072
10	Kuningan	West Java	0.036	0.233	0.072
11	Cirebon	West Java	0.030	0.209	0.063
12	Majalengka	West Java	0.036	0.229	0.070
13	Sumedang	West Java	0.036	0.234	0.073
14	Indramayu	West Java	0.033	0.210	0.063
15	Subang	West Java	0.035	0.224	0.069
16	Purwakarta	West Java	0.029	0.206	0.061
17	Karawang	West Java	0.030	0.200	0.059

18	Bekasi	West Java	0.025	0.177	0.051
19	Bandung Barat	West Java	0.030	0.214	0.065
20	Pangandaran	West Java	0.038	0.231	0.071
21	Kota Bogor	West Java	0.029	0.195	0.058
22	Kota Sukabumi	West Java	0.031	0.212	0.064
23	Kota Bandung	West Java	0.030	0.199	0.059
24	Kota Cirebon	West Java	0.031	0.201	0.060
25	Kota Bekasi	West Java	0.026	0.165	0.047
26	Kota Depok	West Java	0.027	0.176	0.051
27	Kota Cimahi	West Java	0.028	0.191	0.056
28	Kota Tasikmalaya	West Java	0.031	0.207	0.062
29	Kota Banjar	West Java	0.036	0.227	0.070
30	Cilacap	Central Java	0.035	0.232	0.072
31	Banyumas	Central Java	0.036	0.236	0.073
32	Purbalingga	Central Java	0.035	0.233	0.072
33	Banjarnegara	Central Java	0.035	0.229	0.071
34	Kebumen	Central Java	0.037	0.247	0.078
35	Purworejo	Central Java	0.040	0.254	0.081
36	Wonosobo	Central Java	0.035	0.230	0.071
37	Magelang	Central Java	0.036	0.236	0.073

38	Boyolali	Central Java	0.038	0.248	0.078
39	Klaten	Central Java	0.039	0.249	0.079
40	Sukoharjo	Central Java	0.035	0.233	0.072
41	Wonogiri	Central Java	0.044	0.260	0.084
42	Karanganyar	Central Java	0.036	0.235	0.073
43	Sragen	Central Java	0.038	0.244	0.077
44	Grobogan	Central Java	0.035	0.230	0.071
45	Blora	Central Java	0.037	0.240	0.075
46	Rembang	Central Java	0.034	0.225	0.069
47	Pati	Central Java	0.036	0.233	0.072
48	Kudus	Central Java	0.031	0.206	0.062
49	Jepara	Central Java	0.032	0.219	0.067
50	Demak	Central Java	0.030	0.210	0.063
51	Semarang	Central Java	0.035	0.234	0.073
52	Temanggung	Central Java	0.036	0.231	0.071
53	Kendal	Central Java	0.033	0.221	0.067
54	Batang	Central Java	0.033	0.217	0.066
55	Pekalongan	Central Java	0.031	0.217	0.066
56	Pemalang	Central Java	0.033	0.224	0.068
57	Tegal	Central Java	0.032	0.221	0.068

58	Brebes	Central Java	0.032	0.222	0.068
59	Kota Magelang	Central Java	0.036	0.229	0.071
60	Kota Surakarta	Central Java	0.033	0.220	0.067
61	Kota Salatiga	Central Java	0.033	0.227	0.070
62	Kota Semarang	Central Java	0.030	0.205	0.061
63	Kota Pekalongan	Central Java	0.030	0.202	0.060
64	Kota Tegal	Central Java	0.031	0.210	0.063
65	Kulon Progo	Yogyakarta	0.040	0.248	0.078
66	Bantul	Yogyakarta	0.035	0.232	0.072
67	Gunung Kidul	Yogyakarta	0.042	0.253	0.080
68	Sleman	Yogyakarta	0.033	0.223	0.068
69	Kota Yogyakarta	Yogyakarta	0.032	0.215	0.065
70	Pacitan	East Java	0.042	0.252	0.080
71	Ponorogo	East Java	0.041	0.247	0.078
72	Trenggalek	East Java	0.039	0.240	0.075
73	Tulungagung	East Java	0.038	0.237	0.074
74	Blitar	East Java	0.039	0.243	0.076
75	Kediri	East Java	0.036	0.231	0.071
76	Malang	East Java	0.036	0.228	0.070
77	Lumajang	East Java	0.036	0.222	0.068

78	Jember	East Java	0.035	0.224	0.068
79	Banyuwangi	East Java	0.037	0.230	0.071
80	Bondowoso	East Java	0.038	0.227	0.070
81	Situbondo	East Java	0.036	0.218	0.067
82	Probolinggo	East Java	0.034	0.217	0.066
83	Pasuruan	East Java	0.031	0.201	0.060
84	Sidoarjo	East Java	0.029	0.190	0.056
85	Mojokerto	East Java	0.033	0.211	0.063
86	Jombang	East Java	0.034	0.223	0.069
87	Nganjuk	East Java	0.037	0.231	0.072
88	Madiun	East Java	0.041	0.241	0.075
89	Magetan	East Java	0.043	0.251	0.080
90	Ngawi	East Java	0.040	0.236	0.074
91	Bojonegoro	East Java	0.037	0.229	0.071
92	Tuban	East Java	0.035	0.223	0.068
93	Lamongan	East Java	0.037	0.226	0.069
94	Gresik	East Java	0.031	0.201	0.059
95	Bangkalan	East Java	0.032	0.227	0.069
96	Sampang	East Java	0.029	0.211	0.064
97	Pamekasan	East Java	0.031	0.211	0.064

98	Sumenep	East Java	0.036	0.218	0.066
99	Kota Kediri	East Java	0.033	0.212	0.064
100	Kota Blitar	East Java	0.035	0.225	0.069
101	Kota Malang	East Java	0.031	0.211	0.064
102	Kota Probolinggo	East Java	0.032	0.207	0.062
103	Kota Pasuruan	East Java	0.030	0.203	0.060
104	Kota Mojokerto	East Java	0.033	0.209	0.063
105	Kota Madiun	East Java	0.037	0.227	0.070
106	Kota Surabaya	East Java	0.030	0.194	0.057
107	Kota Batu	East Java	0.034	0.221	0.068
108	Pandeglang	Banten	0.029	0.205	0.061
109	Lebak	Banten	0.028	0.194	0.057
110	Tangerang	Banten	0.025	0.172	0.049
111	Serang	Banten	0.027	0.185	0.054
112	Kota Tangerang	Banten	0.026	0.161	0.046
113	Kota Cilegon	Banten	0.026	0.167	0.048
114	Kota Serang	Banten	0.025	0.167	0.048
115	Kota Tangerang Selatan	Banten	0.027	0.169	0.048

Supplementary Table S3: List of transmission scenarios and counterfactual scenarios for model simulations.

Transmission scenarios		
Scenario name	**Details**	**Results shown in**
Rural 100%	R_0 and R_t of urban and rural districts in each province were assumed to be the same.	**Figure S5**
Rural 90%	R_0 and R_t of rural districts were assumed to be 90% of the province level R_0 and R_t. Used as the main transmission scenario shown in the main text.	**Figure 4; Figure S5**
Rural 75%	R_0 and R_t of rural districts were assumed to be 75% of the province level R_0 and R_t.	**Figure S5**
Rural 60%	R_0 and R_t of rural districts were assumed to be 60% of the province level R_0 and R_t.	**Figure S5**

Counterfactual scenarios			
Scenario name	**Details**	**Transmission scenario used**	**Results shown in**
Baseline Scenario	Movement from a district is assumed to reduce according to reductions in movement within a district scaled by an odds ratio of 2 to reflect assumed lower likelihood of long-distance travel.	Rural 90%	**Figure 4; Figure S6 (as a sensitivity analysis comparing to Ramadan mobility scaling with OR=100)**
Ramadan scenario 1	No movement reductions between districts during the Ramadan and Eid festivals period and the R_t values during the period were assumed to be similar to the main/actual scenario.	Rural 90%	**Figure 4**
Ramadan scenario 2	No movement reductions between districts during the Ramadan and Eid festivals period and the R_t values during the period were assumed to be 75% of each district $R_{0,i}$.	Rural 90%	**Figure 4**

Ramadan scenario 3	No movement reductions between districts during the Ramadan and Eid festivals period and the R_t values during the period were assumed to be the same as each district $R_{0,i}$.	Rural 90%	**Figure 4**
Unmitigated	No interventions assumed which implies no movement reductions over all period of simulations with the R_t values to be the same as each district $R_{0,i}$ over the period of simulations.	Rural 90%	**Figure 4; Table 1**

S7. Model fitting to confirmed and suspected COVID-19 deaths and future projection scenarios in all provinces in Java

Estimating the number of deaths from suspected and probable cases in Java provinces

Jakarta reported a time series dataset of the province daily C19P funerals in their official COVID-19 tracker website (https://corona.jakarta.go.id/id/data-pemantauan) (*1*) which includes confirmed/reported and probable COVID-19 deaths (both combined were then defined as suspected deaths). Whilst for the other five provinces in Java, daily time series data of probable deaths are not available. WHO Indonesia situation reports provide a weekly summary of confirmed and probable deaths (which both combined become suspected deaths) in all provinces in Java since the end of May 2020 (**Figure S7**) (*4*). We collated these data and calculated the proportion of confirmed deaths from suspected COVID-19 deaths for each province (ρ_i with i as each province index).

For all days from 1st March 2020, up to 2nd September 2020, we simulated the number of probable deaths in five Java provinces other than Jakarta. Firstly, we aggregated the daily confirmed deaths in each province to a weekly period ($D_{i,t}$ with t as the weekly time window). For each weekly time window t, using Negative Binomial distribution, we simulated the number of probable deaths ($O_{i,t}$) in each province 10 times:

$$O_{i,t} = NB(D_{i,t}, \rho_i).$$

For each simulated $O_{i,t}$, we simulated the spread of the weekly total estimated probable deaths into daily estimated probable deaths using Multinomial distribution, assuming equal probability for all days during the week 10 times:

$$o_{i,t} = Multinom(O_{i,t}, \pi)$$

where π is a vector of length 7, where each value is 1/7.

The simulations resulted in 100 samples of estimated daily probable deaths in each province. Adding the simulated daily probable deaths to the daily confirmed deaths, we obtained 100 samples of the estimated number of daily suspected COVID-19 deaths in five provinces in Java other than Jakarta.

The daily suspected COVID-19 deaths are then defined, for Jakarta, as the daily C19P funerals, and for five other Java provinces as the median of the estimated number of the daily suspected COVID-19 deaths.

Model fitting

Using the framework developed in the Imperial College COVID-19 LMIC reports (*18*), we fit the model to both the daily COVID-19 confirmed deaths and the daily COVID-19 suspected deaths data for each province in Java, estimating both a province-specific R_0 and epidemic start date. To provide model fits that are agnostic to the mobility profiles in each province, we model the time-varying reproduction number, R_t, using a series of pseudo-random walk parameters, which alter the transmission every 2-weeks, with R_t given by:

$$R_t = R_0 \,.\, f(-\rho_1 - \rho_2 \ldots - \rho_n)$$

Where $f(x) = 2\, exp(x)/(1 + exp(x))$, i.e. twice the inverse logit function, which has been used in previous models to capture the impact of mobility data on transmission (*19*). Each ρ parameter is introduced two weeks after the previous parameter, serving to capture changes in transmission over time. More specifically, each ρ parameter is set equal to 0 for each day prior to its start date. For example, ρ_1 is the change in transmission, which is set to start at the beginning of the epidemic. The estimated value for ρ_1 is then maintained for all future time points. ρ_2 is the second change in transmission, which starts 14 days after the epidemic start date, i.e. is equal to 0 prior to this. The last mobility independent change in transmission, ρ_n is maintained for the last 4 weeks prior to the current day to reflect our inability to estimate the effect size of this parameter due to the approximate 21 day delay between infection and death (*16*).

The model fitting results were presented in **Figure S9 & S10**. Based on the fitted models in all provinces considering different types of deaths data, we estimated the attack rate at the province level and Java level.

Future projection scenarios

Using the same modelling framework for the model fitting process, we did forward projections based on scenarios described in **Table S4**.

Supplementary Table S4: List of projection scenarios.

Projection scenarios		
Scenario name	**Details**	**Output**
$R_c = 0.75 \rightarrow 2.00$ (Susp.)	Based on the model fitted to suspected deaths data, forward projections were simulated assuming the R_c dropped to 0.75. Transmission returns to levels observed at the beginning of the outbreak (i.e. $R_c = 2$) due to behaviour change once burden declines to low levels (total deaths for 7 consecutive days < 7).	**Daily number of deaths (Figure 5)**
$R_c = 0.75 \rightarrow 1.25$ (Susp.)	Based on the model fitted to suspected deaths data, forward projections were simulated assuming the R_c dropped to 0.75. Transmission returns to current levels observed during AKB (i.e. $R_c = 1.25$) due to behaviour change and sustained intervention policies once burden declines to low levels (total deaths for 7 consecutive days < 7).	**Daily number of deaths (Figure 5)**
$R_c = 0.75 \rightarrow 1.25$ (Conf.)	Based on the model fitted to suspected deaths data, forward projections were simulated assuming the R_c dropped to 0.75. Transmission returns to current levels observed during AKB (i.e. $R_c = 1.25$) due to behaviour change and sustained intervention policies once burden declines to low levels (total deaths for 7 consecutive days < 7).	**Daily number of deaths (Figure 5)**
$R_c = 1.25 \rightarrow 2.00$ (Susp.)	Based on the model fitted to suspected deaths data, forward projections were simulated assuming the R_c stayed at the current estimated level in all provinces (1.25 - within the range of the most recent point estimates in **Figures S9 & S10**). Transmission returns to levels observed at the beginning of the outbreak (i.e. $R_c = 2$) due to behaviour change once burden declines to low levels (total deaths for 7 consecutive days < 7).	**Daily number of deaths and healthcare demand (Figure 5)**
$R_c = 1.25 \rightarrow 2.00$ (Conf.)	Based on the model fitted to confirmed deaths data, forward projections were simulated assuming the R_c stayed at the current estimated level in all provinces (1.25). Transmission returns to levels observed at the beginning of the outbreak (i.e. $R_c = 2$) due to behaviour change once burden declines to low levels (total deaths for 7 consecutive days < 7).	**Daily number of deaths and healthcare demand (Figure 5)**
$R_c = 2.00$ (Susp.)	Based on the model fitted to suspected deaths data, forward projections were simulated assuming the R_c increased to the initial level of 2.00 in all provinces, representing 'back-to-normal' condition.	**Daily number of deaths (Figure 5)**

S8. Additional supplementary figures

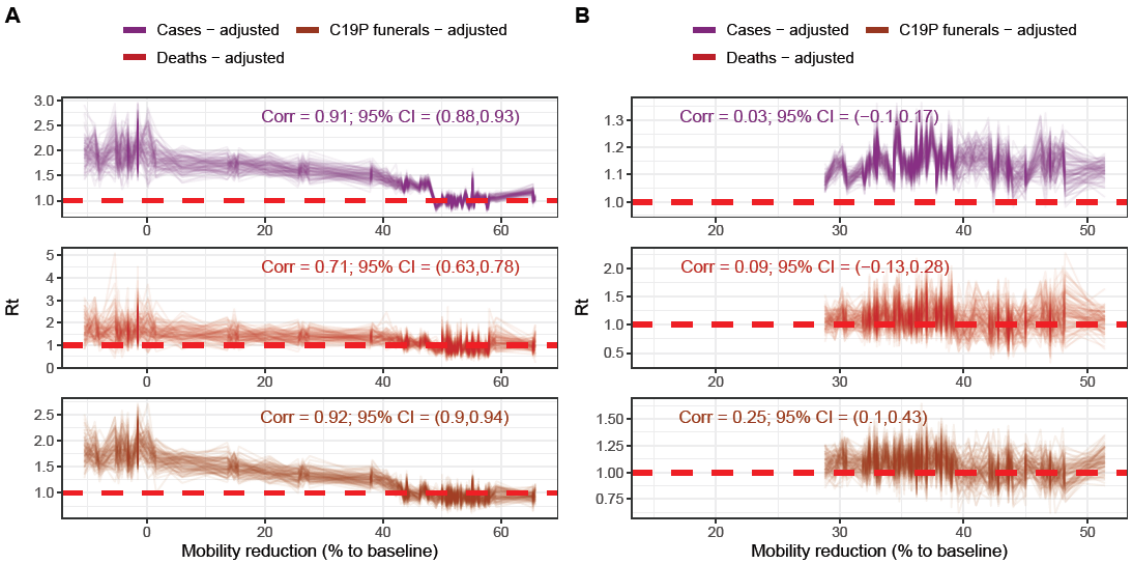

Supplementary Figure S3: Decorrelations between estimated in Jakarta and mobility changes based on estimates before AKB (the 'new normal') **(A)** and after AKB **(B)**.

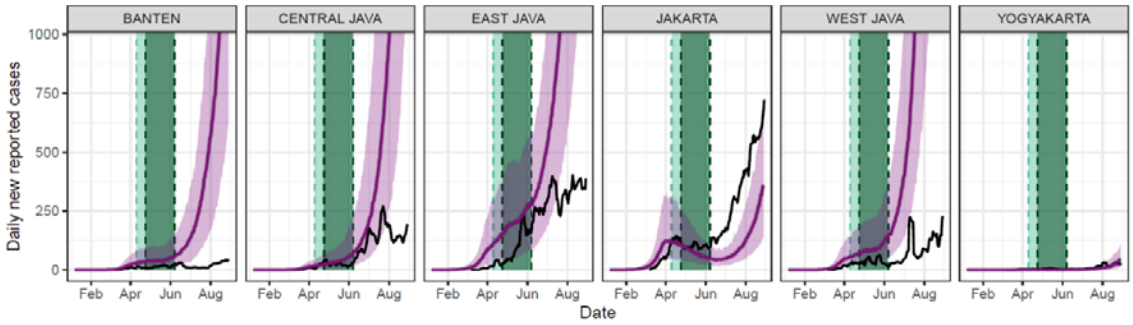

Supplementary Figure S4: Comparison of model simulations and observed daily new reported cases from COVID-19. Coloured lines and their shaded areas denote model simulation outputs with their respective uncertainties (95% level) while black lines denote observed data.

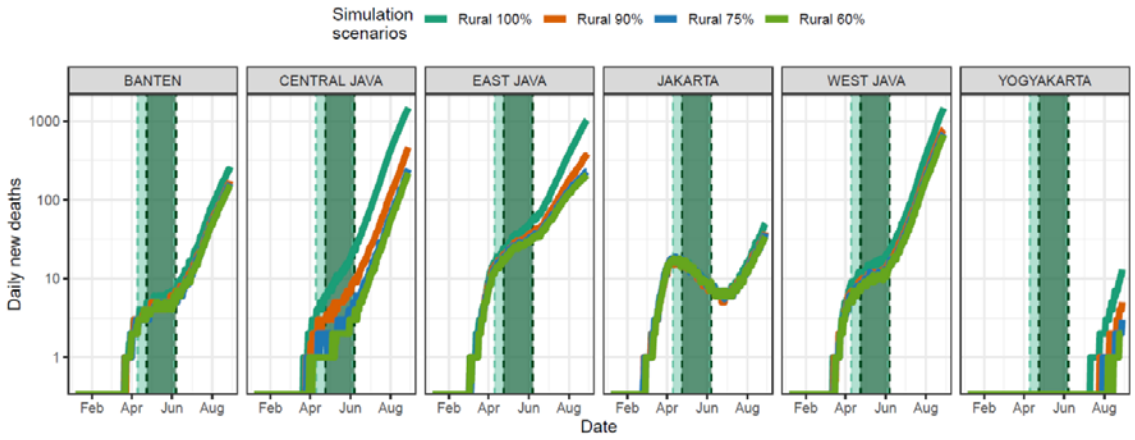

Supplementary Figure S5: Simulated daily new deaths comparing rural transmission scenarios at the province-level.

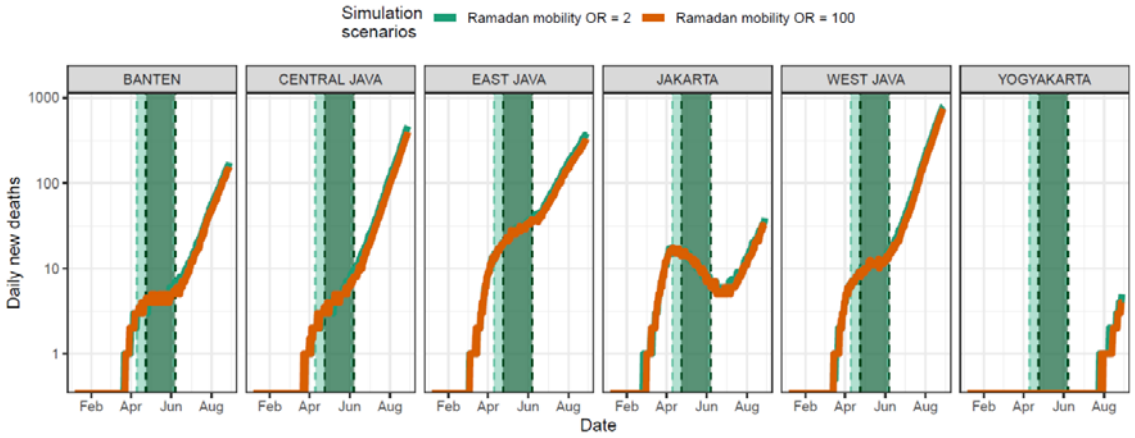

Supplementary Figure S6: Sensitivity analysis for inter-district mobility scaling during Ramadan, with OR=2 (the baseline scenario) and OR=100.

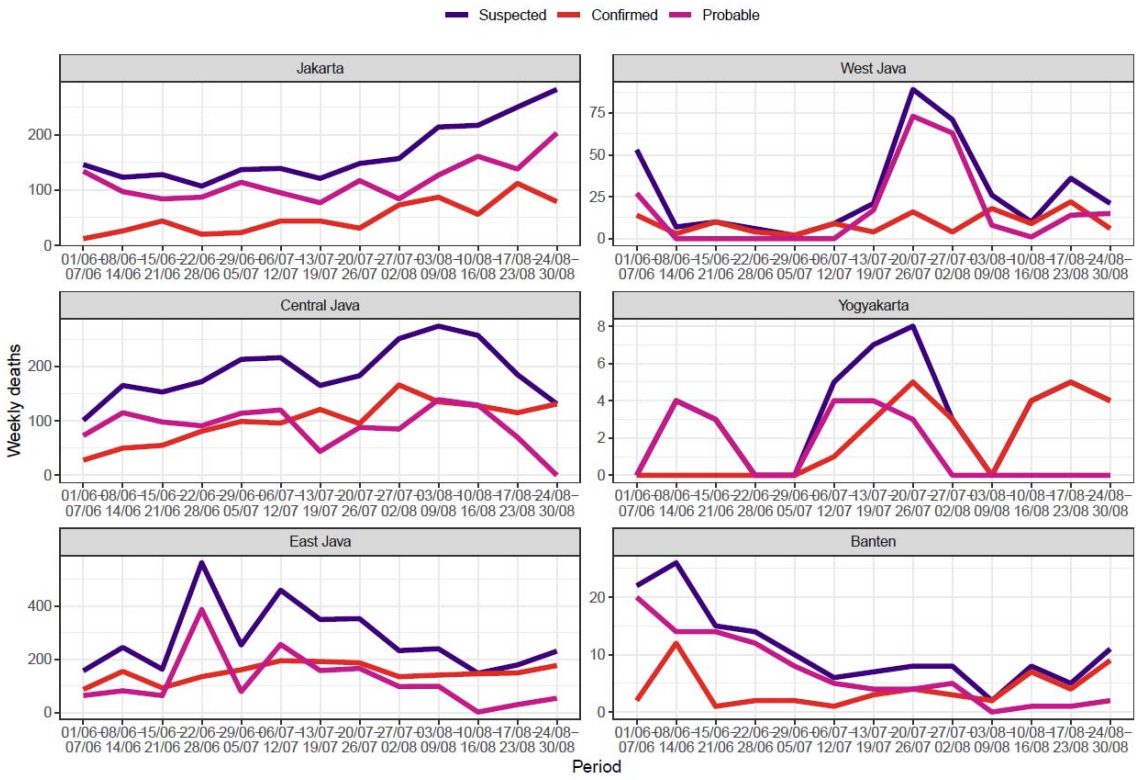

Supplementary Figure S7: Weekly aggregated reported/confirmed and probable deaths in Java collated from WHO COVID-19 Indonesia situation reports 13-23 (*4*).

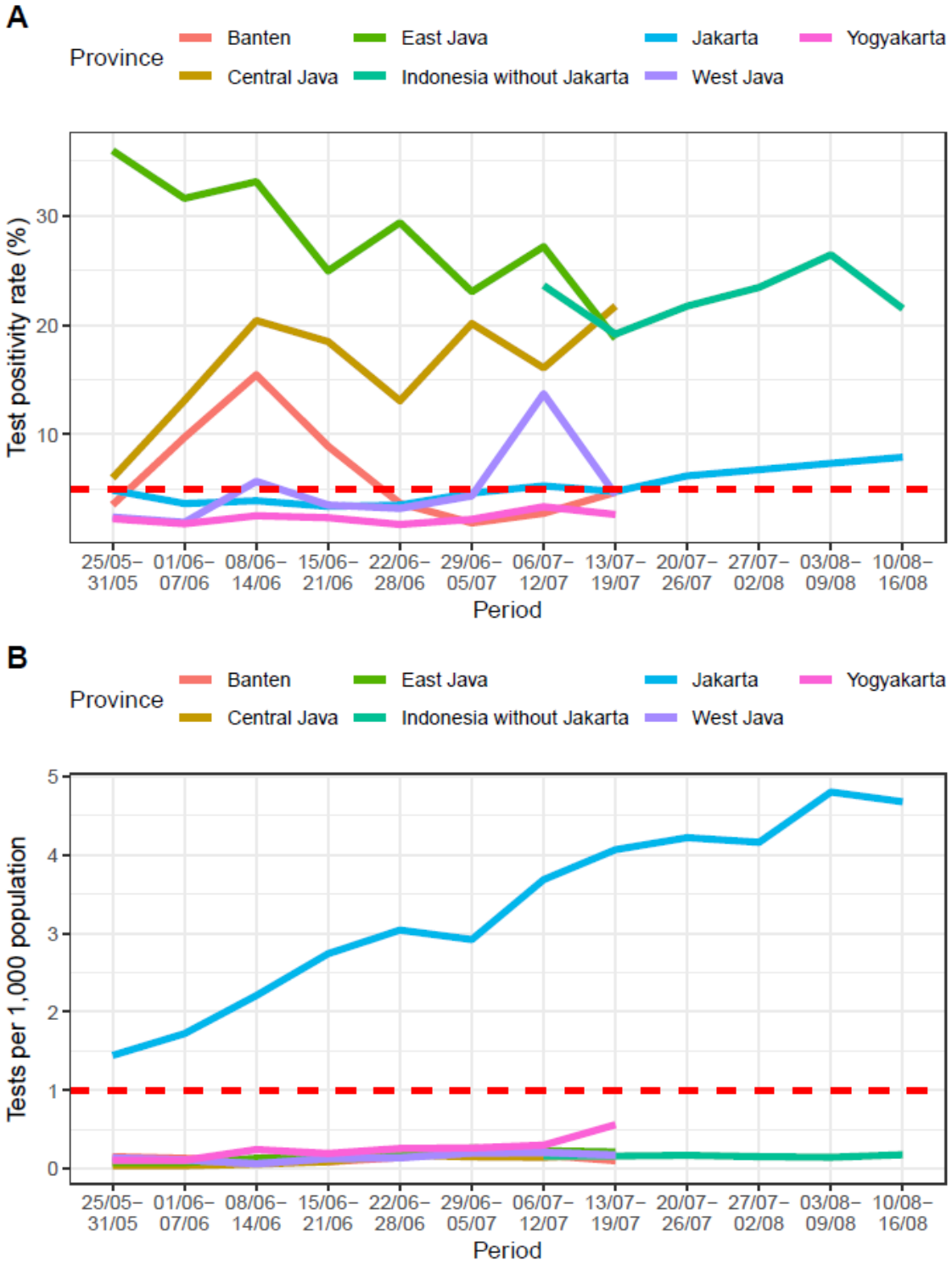

Supplementary Figure S8: Weekly COVID-19 test positivity rates (A) and COVID-19 tests per 1,000 populations in Java collated from WHO COVID-19 Indonesia situation reports 13-23 (*4*).

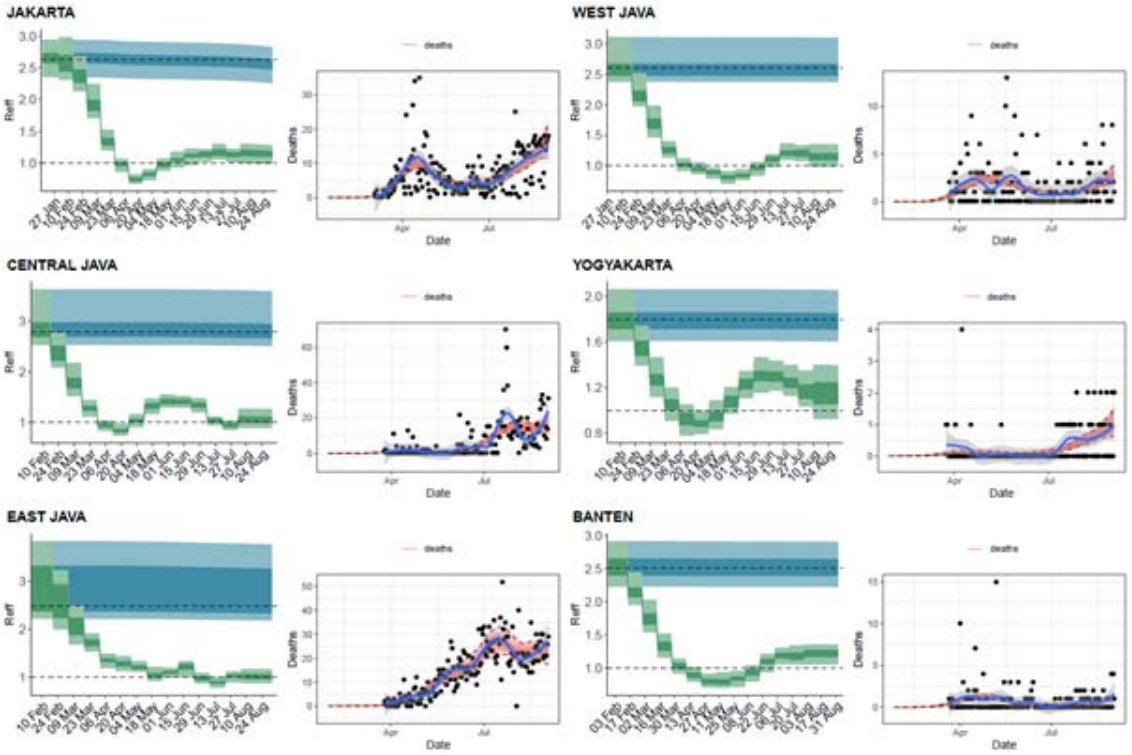

Supplementary Figure S9: Model fits to reported deaths data and estimated values.

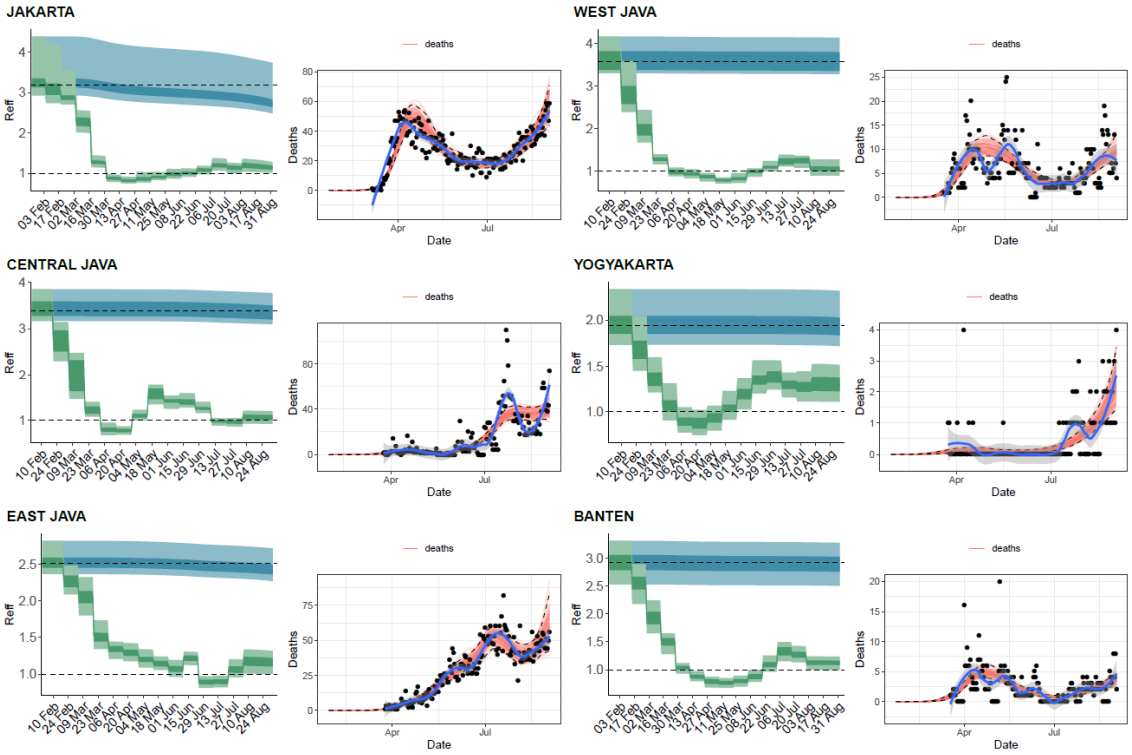

Supplementary Figure S10: Model fits to suspected deaths data and estimated values.

References

1. Jakarta Provincial Health Department, Jakarta COVID-19 Data Monitoring (2020), (available at https://corona.jakarta.go.id/id/data-pemantauan).
2. COVID-19 di Indonesia @kawalcovid19 online spreadsheet (tab: Kasus per Provinsi) (2020), (available at kcov.id/daftarpositif).
3. Satuan Tugas Penanganan COVID-19 (Indonesia COVID-19 Response Acceleration Task Force), Peta Sebaran (2020), (available at https://covid19.go.id/peta-sebaran).
4. WHO Indonesia, COVID-19 Indonesia Situation Reports (2020), (available at https://www.who.int/indonesia/news/novel-coronavirus/situation-reports).
5. Google LLC, Google COVID-19 Community Mobility Reports, (available at https://www.google.com/covid19/mobility/).
6. Directorate General of Health Services Ministry of Health of the Republic of Indonesia, Fasyankes Online, (available at http://sirs.yankes.kemkes.go.id/fo/).
7. Ministry of Health of the Republic of Indonesia, "Ketahanan Kesehatan dalam Menjalani Tatanan Hidup Baru" (Jakarta, 2020).
8. S. Chakraborty, D. Chakravarty, Discrete gamma distributions: Properties and parameter estimations. *Commun. Stat. - Theory Methods.* **41**, 3301–3324 (2012).
9. A. Cori, N. M. Ferguson, C. Fraser, S. Cauchemez, A new framework and software to estimate time-varying reproduction numbers during epidemics. *Am. J. Epidemiol.* **178**, 1505–12 (2013).
10. A. Cori, EpiEstim: A Package to Estimate Time Varying Reproduction Numbers from Epidemic Curves. *R Packag. version 2.2-3* (2020), (available at https://cran.r-project.org/package=EpiEstim).
11. Q. Bi, Y. Wu, S. Mei, C. Ye, X. Zou, Z. Zhang, X. Liu, L. Wei, S. A. Truelove, T. Zhang, W. Gao, C. Cheng, X. Tang, X. Wu, Y. Wu, B. Sun, S. Huang, Y. Sun, J. Zhang, T. Ma, J. Lessler, T. Feng, Epidemiology and transmission of COVID-19 in 391 cases and 1286 of their close contacts in Shenzhen, China: a retrospective cohort study. *Lancet Infect. Dis.* **0** (2020), doi:10.1016/S1473-3099(20)30287-5.
12. M. J. Keeling, L. Danon, M. C. Vernon, T. A. House, Individual identity and movement networks for disease metapopulations. *Proc. Natl. Acad. Sci. U. S. A.* **107**, 8866–8870 (2010).
13. O. J. Watson, P. Walker, C. Whittaker, P. Winskill, G. Charles, squire: SEIR transmission model of COVID-19, (available at https://github.com/mrc-ide/squire).
14. WorldPop, Global Flight Data Annual (2020), , doi:10.5258/SOTON/WP00100.
15. S. A. Lauer, K. H. Grantz, Q. Bi, F. K. Jones, Q. Zheng, H. R. Meredith, A. S. Azman, N. G. Reich, J. Lessler, The Incubation Period of Coronavirus Disease 2019 (COVID-19) From Publicly Reported Confirmed Cases: Estimation and Application. *Ann. Intern. Med.* **172**, 577–582 (2020).
16. P. G. T. Walker, C. Whittaker, O. J. Watson, M. Baguelin, P. Winskill, A. Hamlet, B. A. Djafaara, Z. Cucunubá, D. Olivera Mesa, W. Green, H. Thompson, S. Nayagam, K. E. C. Ainslie, S. Bhatia, S. Bhatt, A. Boonyasiri, O. Boyd, N. F. Brazeau, L. Cattarino, G. Cuomo-Dannenburg, A. Dighe, C. A. Donnelly, I. Dorigatti, S. L. van Elsland, R. FitzJohn, H. Fu, K. A. M. M. Gaythorpe, L. Geidelberg, N. Grassly, D. Haw, S. Hayes, W. Hinsley, N. Imai, D. Jorgensen, E. Knock, D. Laydon, S. Mishra, G. Nedjati-Gilani, L. C. Okell, H. J. Unwin, R. Verity, M. Vollmer, C. E. Walters, H. Wang, Y. Wang, X. Xi, D. G. Lalloo, N. M. Ferguson, A. C. Ghani, The impact of COVID-19 and strategies for mitigation and suppression in low- and middle-income countries. *Science (80-.).* **369**, eabc0035 (2020).
17. Intensive Care National Audit & Research Centre, "ICNARC report on COVID-19 in critical care."
18. Imperial College COVID-19 LMIC Reports. Version 5. MRC Centre for Global Infectious Disease Analysis, Imperial College London. *2020*, (available at https://mrc-ide.github.io/global-lmic-reports/).
19. H. J. T. Unwin, S. Mishra, V. C. Bradley, A. Gandy, T. A. Mellan, H. Coupland, J. Ish-Horowicz,

M. A. C. Vollmer, C. Whittaker, S. L. Filippi, X. Xi, M. Monod, O. Ratmann, M. Hutchinson, F. Valka, H. Zhu, I. Hawryluk, P. Milton, K. E. C. Ainslie, M. Baguelin, A. Boonyasiri, N. F. Brazeau, L. Cattarino, Z. M. Cucunubá, G. Cuomo-Dannenburg, I. Dorigatti, O. D. Eales, J. W. Eaton, S. L. van Elsland, R. G. FitzJohn, K. A. M. Gaythorpe, W. Green, W. Hinsley, B. Jeffrey, E. Knock, D. J. Laydon, J. Lees, G. Nedjati-Gilani, P. Nouvellet, L. C. Okell, K. V Parag, I. Siveroni, H. A. Thompson, P. Walker, C. E. Walters, O. J. Watson, L. K. Whittles, A. Ghani, N. M. Ferguson, S. Riley, C. A. Donnelly, S. Bhatt, S. Flaxman, *medRxiv*, in press, doi:10.1101/2020.07.13.20152355.